

# **The Laramide Caborca Orogenic Gold Belt of Northwestern Sonora, Mexico: White Mica $^{40}\text{Ar}/^{39}\text{Ar}$ Geochronology from Gold-Rich Quartz Veins**

Open-File Report 2016–1008



# **The Laramide Caborca Orogenic Gold Belt of Northwestern Sonora, Mexico: White Mica $^{40}\text{Ar}/^{39}\text{Ar}$ Geochronology from Gold- Rich Quartz Veins**

By Aldo Izaguirre, Michael J. Kunk, Alexander Iriondo, Ryan McAleer, Juan Antonio Caballero-Martínez, and Enrique Espinosa-Arámburu

Open-File Report 2016–1008

**U.S. Department of the Interior  
U.S. Geological Survey**

**U.S. Department of the Interior**  
SALLY JEWELL, Secretary

**U.S. Geological Survey**  
Suzette M. Kimball, Director

U.S. Geological Survey, Reston, Virginia: 2016

For more information on the USGS—the Federal source for science about the Earth, its natural and living resources, natural hazards, and the environment—visit <http://www.usgs.gov> or call 1-888-ASK-USGS.

For an overview of USGS information products, including maps, imagery, and publications, visit <http://www.usgs.gov/pubprod/>.

Any use of trade, firm, or product names is for descriptive purposes only and does not imply endorsement by the U.S. Government.

Although this information product, for the most part, is in the public domain, it also may contain copyrighted materials as noted in the text. Permission to reproduce copyrighted items must be secured from the copyright owner.

Suggested citation:

Izaguirre, Aldo, Kunk, M.J., Iriondo, Alexander, McAleer, Ryan, Caballero-Martínez, J.A, and Espinosa Arámburu, Enrique, 2016, The Laramide Caborca orogenic gold belt of northwestern Sonora, Mexico; white mica  $^{40}\text{Ar}/^{39}\text{Ar}$  geochronology from gold-rich quartz veins: U.S. Geological Survey Open-File Report 2016-1008, 30 p., <http://dx.doi.org/10.3133/ofr20161008>.

## Contents

|  |   |
|--|---|
| 1. Introduction .....  | 1 |
| 2. Methods .....   | 2 |
| 2.1. Sample Preparation .....                                  | 2 |
| 2.2. Packing and Irradiation Method .....                      | 2 |
| 2.3. Sample Analysis.....                                      | 2 |
| 2.4. Isotopic Data Reduction .....                             | 3 |
| 3. Results of $^{40}\text{Ar}/^{39}\text{Ar}$ Data.....        | 3 |
| 3.1. Group 1 Plateau Ages .....                                | 3 |
| 3.2. Group 2 Isochron Ages .....                               | 3 |
| 3.3. Group 3 Average or Single-Step Ages .....                 | 3 |
| 3.4. Histogram and Cumulative Probability Diagram of Ages..... | 4 |
| 4. Conclusions .....   | 4 |
| 5. Acknowledgments.....  | 4 |
| 6. References Cited .....                                      | 5 |

## Figures

|   |    |
|---|----|
| 1. Sample locations for dated white micas of gold-rich quartz veins.....  | 7  |
| 2. Histogram and cumulative probability distribution diagram of $^{40}\text{Ar}/^{39}\text{Ar}$ ages determined from hydrothermal white mica samples of gold-rich quartz veins from the Caborca orogenic gold belt (COGB), northwestern Sonora, Mexico..... | 8  |
| 3. Age spectra and inverse-isotope correlation diagrams from group 1 of white mica samples of gold-rich quartz veins, with plateau ages as best age, from the Caborca orogenic gold belt (COGB), northwestern Sonora, Mexico.....                           | 9  |
| 4. Age spectra and inverse-isotope correlation diagrams from group 2 of white mica samples of gold-rich quartz veins, with isochron ages as best age, from the Caborca orogenic gold belt (COGB), northwestern Sonora, Mexico.....                          | 16 |
| 5. Age spectra and inverse-isotope correlation diagrams from group 3 of white mica samples of gold-rich quartz veins, with average and (or) single-step ages as best age, from the Caborca orogenic gold belt (COGB), northwestern Sonora, Mexico.....      | 22 |

## Tables

[Available as separate files for download in Excel format from <http://dx.doi.org/10.3133/ofr20161008>.]

1. Summary of 63  $^{40}\text{Ar}/^{39}\text{Ar}$  ages determined from white micas of gold-rich quartz veins of the Caborca orogenic gold belt (COGB), northwestern Sonora, Mexico.
2.  $^{40}\text{Ar}/^{39}\text{Ar}$  step-heating data and plateau ages determined from white micas of gold-rich quartz veins of the Caborca orogenic gold belt (COGB), northwestern Sonora, Mexico.
3.  $^{40}\text{Ar}/^{39}\text{Ar}$  step-heating data and isochron ages determined from white micas of gold-rich quartz veins of the Caborca orogenic gold belt (COGB), northwestern Sonora, Mexico.
4.  $^{40}\text{Ar}/^{39}\text{Ar}$  step-heating data and average or single step ages determined from white micas of gold-rich quartz veins of the Caborca orogenic gold belt (COGB), northwestern Sonora, Mexico.

## Conversion Factors

| Multiply       | By     | To obtain |
|----------------|--------|-----------|
|                | Length |           |
| kilometer (km) | 0.6214 | mile (mi) |

Temperature in degrees Celsius ( $^{\circ}\text{C}$ ) may be converted to degrees Fahrenheit ( $^{\circ}\text{F}$ ) as follows:  
 $^{\circ}\text{F}=(1.8\times^{\circ}\text{C})+32$

# The Laramide Caborca Orogenic Gold Belt of Northwestern Sonora, Mexico: White Mica $^{40}\text{Ar}/^{39}\text{Ar}$ Geochronology from Gold-Rich Quartz Veins

By Aldo Izaguirre,<sup>1,2</sup> Michael J. Kunk,<sup>3</sup> Alexander Iriondo,<sup>2,4</sup> Ryan McAleer,<sup>3</sup> Juan Antonio Caballero-Martínez,<sup>5</sup> and Enrique Espinosa-Arámburu<sup>5</sup>

## 1. Introduction

This report contains reduced  $^{40}\text{Ar}/^{39}\text{Ar}$  geochronological data from hydrothermal white mica (63 samples) separated from orogenic quartz gold-rich veins in the Laramide Caborca orogenic gold belt (COGB) of northwestern Sonora, Mexico (fig. 1). The main objective of this report is to present the sample locations,  $^{40}\text{Ar}/^{39}\text{Ar}$  experimental methodology, and  $^{40}\text{Ar}/^{39}\text{Ar}$  isotopic data (tables 1–4). We also include age spectra and inverse-isotope correlation diagrams for all white mica samples (figs. 3–5). The age spectra are separated into three groups based on the type of age used for geologic interpretation, including (1) plateau ages, (2) isochron ages, and (3) average or single-step heating ages. These age spectra are interpreted to represent the time of mineralization for each sample locality, and together, all the ages help to establish the age of mineralization for the entire COGB (fig. 2). Another objective of this Open-File Report (OFR) is to organize the data in a systemic way so that they can be integrated into future scientific publications.

The COGB is approximately 600 kilometers (km) long and 60 to 80 km wide, trends northwest, and extends from west-central Sonora to southern Arizona and California (fig. 1). The COGB contains mineralized gold-rich quartz veins that contain free gold associated with white mica “sericite” and carbonate minerals (calcite and ankerite) plus sulfides such as pyrite and galena (Izaguirre and others, 2012).

Limited geochronologic studies (K-Ar, Ar-Ar (white mica), and Re-Os (magnetite)) exist for parts of the COGB, and previous work was concentrated in mining districts (Pérez-Segura, 1993; Pérez-Segura and others, 1996; Araux-Sánchez, 2000; Iriondo and Atkinson, 2000; Iriondo, 2001; Poulsen and others, 2008; Quintanar-Ruiz, 2008). These scattered studies recorded mineralization ages of approximately 70 to 40 Ma (mega-annum, or million years ago). Therefore, some workers proposed that the orogenic gold mineralization in the region occurred during a single pulse that was associated with the Laramide Orogeny that took place during Cretaceous to early Eocene in the western margin of North America (Damon and others, 1964; Coney, 1976; Dickinson and others, 1988). However, the geochronologic dataset was quite limited, making any regional interpretations tenuous. Accordingly, one of the objectives of this geochronology study was to get a better representative sampling of the COGB in order to obtain a more complete record of the mineralization history. The 63 samples presented in this work are broadly distributed throughout the area of the COGB (fig. 1) and allow us to better test the hypothesis that mineralization occurred in a single pulse.

---

<sup>1</sup>U.S. Geological Survey, Mail Stop 973, Denver Federal Center, Denver, CO 80225

<sup>2</sup>Centro de Geociencias, Universidad Nacional Autónoma de México, Campus Juriquilla, Boulevard Juriquilla 3001, Juriquilla, 76230, Querétaro, México

<sup>3</sup>U.S. Geological Survey, Mail Stop 926A, National Center, Reston, VA 20192

<sup>4</sup>Department of Geological Sciences, Jackson School of Geosciences, The University of Texas at Austin, Austin, TX 78712

<sup>5</sup>Servicio Geológico Mexicano, Boulevard Felipe Ángeles, km 93.50-4, Colonia Venta Prieta, 42080, Hidalgo, México

## 2. Methods

### 2.1. Sample Preparation

All of the quartz vein samples were crushed, ground, and sized using 250-, 180-, and 150-micrometer ( $\mu\text{m}$ ) sieves. White mica separations were performed using a magnetic separation instrument (Frantz<sup>TM</sup>), paper shaking, and hand picking with a goal of getting greater than 99 percent purity on the white mica. The resulting separates were washed three times in acetone, alcohol, and deionized water in an ultrasonic cleaner (Branson<sup>TM</sup>) to remove dust and other impurities, and then re-sieved using 250- and 180- $\mu\text{m}$  sieve sizes.

### 2.2. Packing and Irradiation Method

The samples were irradiated in five separate irradiation packages (DD60, KD12, KD52, KD53, and KD55). Two copper packets were loaded for each white mica sample, with weights of approximately 1 milligram (mg) and 20 mg, respectively. The packets were sealed under vacuum in fused silica tubes and irradiated in the central thimble facility at the Training Reactor Isotopes General Atomics (TRIGA) reactor at the U.S. Geological Survey in Denver, Colorado. The monitor mineral used in all the irradiation packages was hornblende (sample MMhb-1) with an age of  $519.4 \pm 2.5$  Ma (Alexander and others, 1978; Dalrymple and others, 1981). The type of container, and the geometry of samples and standards are similar to those described by Sneek and others (1988).

### 2.3. Sample Analysis

White mica samples were analyzed in the U.S. Geological Survey Argon Thermochronology Laboratory in Reston, Virginia. The large white mica samples (approximately 20 mg) were analyzed in a VG Isotopes, Ltd. model 1200 mass spectrometer fitted with an electron multiplier using the  $^{40}\text{Ar}/^{39}\text{Ar}$  step-heating method. All samples were heated for 10 minutes per step (11–20 steps) in a small-volume, molybdenum-lined, low-blank tantalum resistance furnace similar to that described by Staudacher and others (1978). The temperature was monitored by a W5Re-W26Re thermocouple and controlled by a proportional, programmable controller. The furnace and the rear manifold were pumped between steps with a turbo molecular pump. Two isolated ion pumps evacuated the front manifold and the mass spectrometer flight-tube between each incremental step. Prior to analysis in the mass spectrometer, the gas was purified in the rear manifold by a SAES ST707 Zr-V-Fe (zirconium-vanadium-iron) getter operated at room temperature and a hot Re (rhenium) filament. Gas was equilibrated with the front manifold, then isolated and cleaned in the front manifold with a SAES ST101 Al-Zr (aluminum-zirconium) getter operated at 400°C and a Ti (titanium) getter operated at 350°C.

An activated charcoal finger submerged in a thermally equilibrated mixture of dry ice and acetone in the front manifold was used to remove gasses with a molecular weight greater than 60 or 80 (primarily other noble gasses) prior to the expansion of the Ar (argon) dominated gas into the mass spectrometer. The gas was further purified in the mass spectrometer by a second SAES ST101 getter operated at room temperature. Ar isotopes with atomic weights of 40 through 36 and  $\text{CO}_2$  (atomic weight of 44) were analyzed as a function of time in five or six analytical cycles.  $^{40}\text{Ar}$ ,  $^{39}\text{Ar}$ ,  $^{38}\text{Ar}$ , and  $^{37}\text{Ar}$  peaks and their baselines were measured for five, 1.28-second integrations in each of the five cycles.  $^{36}\text{Ar}$  and its baselines were measured for twenty, 1.28-second integrations in each cycle. After the analysis, the mass spectrometer was evacuated with an isolated ion pump. All phases of the sample heating, cleanup, equilibration, and analysis were performed under computer automation.

Smaller white mica samples (weights of approximately 1 mg) were analyzed using a MAP-216 mass spectrometer fitted with an electron multiplier using the  $^{40}\text{Ar}/^{39}\text{Ar}$  step-heating dating method. Heating for 10 minutes per step followed a schedule of 11 to 20 steps. The heating schedules were designed such that the percentage of  $^{39}\text{Ar}$  released per step was limited to less than 20 percent of the total released for most samples. The samples were heated in the same manner and in the same type of furnace as was described earlier. The furnace and the rear and front manifolds were pumped between steps with a turbo molecular pump. An isolated ion pump was used to pump the mass spectrometer. Prior to the mass spectrometer analysis, the gas was purified in the manifold by two SAES ST101 Al-Zr getters, one operated at room temperature and a second one using a hot Re filament at 400°C. The Ar-rich gas was further purified by a third SAES ST101 getter operated at room temperature in the flight tube of the mass spectrometer. Ar isotopes with atomic weights of 40 through 36 were analyzed as a function of time in six analytical cycles. Baselines were measured for  $^{39}\text{Ar}$  and  $^{36}\text{Ar}$ . The  $^{36}\text{Ar}$  baselines were subtracted from the  $^{40}\text{Ar}$ ,  $^{38}\text{Ar}$ ,  $^{37}\text{Ar}$ , and  $^{36}\text{Ar}$  peaks. The  $^{39}\text{Ar}$  baseline was subtracted from the  $^{39}\text{Ar}$  peak to reduce the influence of the tail of the  $^{40}\text{Ar}$  peak.

## 2.4. Isotopic Data Reduction

All the isotopic data produced on the VG-1200 spectrometer were reduced using an updated version of the computer program ArAr\* (Haugerud and Kunk, 1988). Isotopic data from the MAP-216 spectrometer was reduced using the computer program Mass Spec (Deino, 2001). We used the decay constants recommended by Steiger and Jäger (1977). The isotopic measurements made in the five- or six-cycle analysis were regressed to time zero (2/3 of the inlet time) using standard linear regression techniques. These regressed peak values, and associated analytical uncertainties, were used in data reduction. For the VG-1200 and the MAP-216, full system blanks were measured prior to the suite of analyses made on each sample and then subtracted from the analytical results. Error estimates of the blanks were quadratically combined with the analytical errors.

Corrections for interfering reactor-produced Ar isotopes from Ca (calcium), K (potassium), and Cl (chlorine) in the sample were made using the production ratios given in Dalrymple and others (1981) and Roddick (1983). Errors in calculated ages or ratios include the measurement uncertainty in the analysis, decay factor uncertainties, uncertainties in measured atmospheric  $^{40}\text{Ar}/^{36}\text{Ar}$  ratios, the irradiation parameter J, the production ratios of the various reactor induced Ar producing reactions, the initial  $^{38}\text{Ar}/^{36}\text{Ar}$  ratio, and the age of the monitor mineral (Haugerud and Kunk, 1988).

The data in tables 2, 3, and 4 include individual step ages and total gas ages. Total gas ages represent the age calculated from the addition of all the measured Ar peaks for all steps in a single sample. The total gas ages are roughly equivalent to conventional K/Ar ages; however, no analytical precision is calculated for these total gas ages.

## 3. Results of $^{40}\text{Ar}/^{39}\text{Ar}$ Data

White mica  $^{40}\text{Ar}/^{39}\text{Ar}$  geochronological results of 63 samples presented in this report (tables 1–4 and figs. 3–5) are subdivided into the following three age groups: plateau ages (group 1), isochron ages (group 2), and average or single-step ages (group 3). The reported ages are plotted in figure 1, and improve our knowledge of the timing of hydrothermal gold-rich quartz vein formation in the COGB.

### 3.1. Group 1 Plateau Ages

Group 1 is made up of 21 samples (tables 1 and 2; fig. 3) of coarse flakes of white mica separated to an optical purity of greater than 99 percent. The data from step-heating experiments on these samples meet the criteria for a plateau age defined by Fleck and others (1977) and modified by Haugerud and Kunk (1988). All of the white mica samples in this group released argon  $^{39}\text{Ar}_k$  in three steps or more (accounting for a minimum of 50 percent of the total released gas) at furnace temperatures between approximately 800 to 1250°C (sample Quitovac-5; fig. 3U). In addition, isochron ages calculated for these samples, shown in inverse isotope diagrams of  $^{36}\text{Ar}/^{40}\text{Ar}$  vs.  $^{39}\text{Ar}/^{40}\text{Ar}$  (sample Quitovac-5; fig. 3V), support within analytical error, the more precise plateau ages (summarized in table 1). Therefore, these white mica plateau ages that range from approximately 66 to 48 Ma are interpreted to be the best approximation for the age of hydrothermal activity that resulted in this group of gold-rich quartz veins.

### 3.2. Group 2 Isochron Ages

Group 2 is made up of 16 samples (tables 1 and 3; fig. 4). White mica from these samples includes both coarse flakes and fine-grained aggregates, separated to an optical purity of greater than 99 percent. The flat age spectra from step-heating experiments on these samples did not meet the statistical definition of a plateau (Fleck and others; 1977). For these slightly irregular age spectra (sample Trin-10; fig. 4AC), inverse isotope correlation diagrams of  $^{36}\text{Ar}/^{40}\text{Ar}$  vs.  $^{39}\text{Ar}/^{40}\text{Ar}$  were generated and isochron ages calculated. A regression (and the resulting age) is considered meaningful if it includes more than three contiguous heating steps that accounts for at least 50 percent of the total  $^{39}\text{Ar}_k$  released and has a MSWD (mean square weighted deviation) of  $\leq 2.5$ . The age range determined for this group of white micas is approximately 62 to 36 Ma, and interpreted as the age interval for hydrothermal mineralization along the COGB.

### 3.3. Group 3 Average or Single-Step Ages

Group 3 is made up of 26 samples of white mica (tables 1 and 4; fig. 5) that consist of mostly fine-grained aggregates of white mica. These samples were prepared to a variety of purity levels (in a few instances less than 99 percent purity). It is possible that many of the impurities in the white mica separates included quartz, plagioclase, K-feldspar, or even igneous or metamorphic white micas from the quartz vein host rocks. These impurities made the  $^{40}\text{Ar}/^{39}\text{Ar}$  data results more difficult to interpret.

## 4 The Caborca Orogenic Gold Belt of Sonora, Mexico: Mica $^{40}\text{Ar}/^{39}\text{Ar}$ Geochronology from Gold-Rich Veins

The data for group 3 white mica samples did not meet the statistical criteria for a plateau or isochron age. However, for a group of 15 of these samples we calculated average ages for a set of contiguous steps (selected steps provided in figure 5). The selected steps define a flat portion of each age (spectrum similar to a plateau), but failed to meet one or more of the requirements established by Fleck and others (1977). This behavior is well represented in white mica sample Pit-4 (fig. 5A1) where 6 steps, representing 87 percent of the total  $^{39}\text{Ar}_k$  released, were used to calculate the weighted-average age. The resulting weighted-average ages are very similar to the calculated total gas ages for the same samples. This group of 15 white micas yielded average ages in a range between approximately 65 to 39 Ma, consistent with the ages determined from groups 1 and 2.

For the remaining 11 samples from group 3 the age of a single-step was used as the preferred age (ages summarized in table 1). The resulting age spectra from these 11 samples are difficult to interpret meaningfully from the step heating results, but it is important to illustrate that not all the  $^{40}\text{Ar}/^{39}\text{Ar}$  data for these gold-rich quartz veins is considered “well behaved” or “ideal,” which would generally yield a flat spectrum. A good example of a “non-ideal” staircase age spectrum is shown in figure 5S (sample El Chanate) in which step C is selected as the assigned age of the sample. The single-step ages of the 11 samples are chosen by selecting the first heating step of the staircase age spectrum in which we observe a tendency of the spectrum to flatten out. The selected single-step age is interpreted as representing the maximum possible age for the formation of the white mica.

Group 3 average and single-step ages range from approximately 69 to 39 Ma. The resulting age spectrum data from group 3 are more complex than groups 1 and 2, however, the determined ages are consistent with the more reliable ages of groups 1 and 2.

### 3.4. Histogram and Cumulative Probability Diagram of Ages

In order to evaluate and interpret the resulting  $^{40}\text{Ar}/^{39}\text{Ar}$  data of the 63 white mica samples, we generated a histogram and a cumulative probability diagram (fig. 2) of all the determined ages. The diagram shows the age range as well as apparent ages of more abundant gold mineralization along the COGB. The Late Cretaceous to late Eocene age range (69 to 36 Ma) for the quartz veins represents a mineralization event that lasted for more than 30 million years. However, in the histogram a probability peak at approximately 61 Ma is interpreted as the climax of mineralization. The climax of mineralization at 61 Ma occurred within the main pulse of mineralization between approximately 63 to 56 Ma (age range of the majority of analyzed white mica samples; 35 white micas and approximately 56 percent of the total samples). After approximately 48 Ma, only 5 scattered ages of mineralization are identified in figure 2. The youngest age is 36 Ma and represents the youngest mineralization age determined for the gold veins along the COGB.

## 4. Conclusions

Organization of this large  $^{40}\text{Ar}/^{39}\text{Ar}$  dataset into three age groups has facilitated the interpretation of the timing of mineralization of gold-rich quartz veins in the COGB (table 1). The data presented in this report will serve as a data repository to facilitate the integration of the age data in future manuscripts for publication in scientific journals, where space restrictions are common.

We conclude that the ages between approximately 69 to 36 Ma (figs. 1 and 2), determined from the 63 white micas, represent the timing of orogenic gold mineralization in northwestern Sonora, Mexico, supporting previous interpretations that these gold-rich quartz veins are restricted to the Late Cretaceous to Eocene time. The vast majority of the sample ages (>56 percent) were determined to be between approximately 63 to 56 Ma, which we interpret as the climax of gold mineralization along the COGB. Moreover, the frequency of mineralization gradually decreased from approximately 56 to 48 Ma, followed by a final stage of vein formation that occurred between approximately 45 to 36 Ma. The end of mineralization most likely relates to the contemporaneous cessation of the Laramide orogeny along this portion of the North American Cordillera.

## 5. Acknowledgments

We acknowledge Consejo Nacional de Ciencia y Tecnología (CONACyT) for providing a doctoral scholarship to Aldo Izaguirre. Also we are grateful to CONACyT for supporting scientific projects CB-82518 and CB-129370 and for financing part of this work. Furthermore, we would like to thank Universidad Nacional Autónoma de México grant PAPIIT IN-116709. We are thankful to the Servicio Geológico Mexicano (SGM) Gerencia Hermosillo, Sonora, for help in the logistics to undertake fieldwork, and in particular, we would like to thank Javier Hernández-Rojas (former SGM geologist) for his helpful companionship in the field while Aldo Izaguirre collected the samples of gold-rich quartz veins. Thanks to Bethany Stackhouse and Wright Horton Jr., for reviewing and improving this manuscript.

## 6. References Cited

- Alexander, E.C., Jr., Mickelson, G.M., and Lanphere, M.A., 1978, MMhb-1—A new  $^{40}\text{Ar}/^{39}\text{Ar}$  dating standard, *in* Zartman, R.E., ed., Short Papers of the Fourth International Conference, Geochronology, Cosmochronology, and Isotope Geology: U.S. Geological Survey Open-File Report 78-701, p. 6-8.
- Araux-Sánchez, E., 2000, Geology and mineral deposits of the Sierra Pinta municipality of Puerto Peñasco, Sonora: Unpublished M.S. thesis, Department of Geology, University of Sonora, Mexico, 121 p.
- Coney, P.J., 1976, Plate tectonics and the Laramide orogeny, *in* Woodward, L.A., and Northrop, S.A., eds., Tectonics and mineral resources of southwestern North America: New Mexico Geological Society Special Publication 6, p. 5-10.
- Dalrymple, G.B., Alexander, E.C., Jr., Lanphere, M.A., and Kraker, G.P., 1981, Irradiation of samples for  $^{40}\text{Ar}/^{39}\text{Ar}$  dating using the Geological Survey TRIGA reactor: U.S. Geological Survey Professional Paper 1176, 55 p. [Also available at <http://pubs.er.usgs.gov/publication/pp1176>.]
- Damon, P.E., Mauger, R.L., and Bikerman, M., 1964, K-Ar dating of Laramide plutonic and volcanic rocks within the Basin and Range province of Arizona and Sonora, *in* Sastry, M.V.A., Bhatia, S.B., eds., Cretaceous-Tertiary boundary including volcanic activity: 22nd Indian Geotechnical Conference, New Delhi, India, Part 3 Proceedings of Section 3, p. 45-55.
- Deino, A.L., 2001, User's manual for mass spec v. 5.02: Berkeley Geochronology Center Special Publication 1a, 119 p.
- Dickinson, W.R., Klute, M.A., Hayes, M.J., Janecke, S.U., Lundin, E.R., McKittrick, M.A., and Olivares, M.D., 1988, Paleogeographic and paleotectonic setting of Laramide sedimentary basins in the central Rocky Mountain region: Geological Society of America Bulletin, v. 100, no. 7, p. 1023-1039.
- Fleck, R.J., Sutter, J.F., and Elliot, D.H., 1977, Interpretation of discordant  $^{40}\text{Ar}/^{39}\text{Ar}$  age spectra of Mesozoic tholeiites from Antarctica: *Geochimica et Cosmochimica Acta*, v. 41, no. 1, p. 15-32.
- Haugerud, R.A., and Kunk, M.J., 1988, ArAr\*; a computer program for reduction of  $^{40}\text{Ar}-^{39}\text{Ar}$  data: U. S. Geological Survey Open-File Report 88-261, 68 p. [Also available at <http://pubs.er.usgs.gov/publication/ofr88261>.]
- Iriondo, A., 2001, Proterozoic basements and their laramide juxtaposition in NW Sonora, Mexico; tectonic constraints on the SW margin of Laurentia: Boulder, Colorado, University of Colorado, unpublished Ph.D. thesis, 3 pls., 222 p.
- Iriondo, A., and Atkinson, W.W., Jr., 2000, Orogenic gold mineralization along the proposed trace of the Mojave-Sonora megashear; evidence for the Laramide Orogeny in NW Sonora, Mexico [abs.]: Geological Society of America Abstracts with Programs, v. 32, no. 7, p. 393
- Izaguirre, A., Iriondo, A., Caballero-Martínez, J.A., Moreira-Rivera, F., and Espinosa-Arámburu, E., 2012, Geochemical homogeneity of hydrothermal alteration of the orogenic gold belt in NW Sonora, Mexico; study of mass balance in host rocks of mineralization: *Bulletin of the Mexican Geological Society*, v. 64, p. 119-153.
- Pérez-Segura, E., 1993, Deposits of gold and silver from Sonora, Mexico and its relations with the regional geology, *in* Delgado-Argote, L.A., and Barajas, M., eds., Contributions to the tectonics of western Mexico: Mexican Geophysical Union Monograph 1, p. 147-174.
- Pérez-Segura, E., Cheilletz, A., Herrera-Urbina, S., and Hanes, Y.J., 1996, Geology, mineralization, hydrothermal alteration, and age of the San Francisco, Sonora gold deposit; a mesothermal deposit in northwestern Mexico: *Mexican Journal of Geological Sciences*, v. 13, no. 1, p. 65-89.
- Poulsen, K.H., Mortensen J.K., and Walford, P.C., 2008, San Francisco gold deposit, Santa Ana region, Sonora, Mexico; Laramide orogenic, intrusion-related mineralization?, *in* Spencer, J.E., and Titley, S.R., eds., Ores and orogenesis; Circum-Pacific tectonics, geologic evolution, and ore deposits: Arizona Geological Society Digest 22, 547-559, available at [http://www.azgs.az.gov/Resources/ags22\\_tablecontents.pdf](http://www.azgs.az.gov/Resources/ags22_tablecontents.pdf).
- Quintanar-Ruíz, F.J., 2008, La Herradura ore deposit; an orogenic gold deposit in northwestern Mexico: Unpublished M.S. thesis, Tucson, Arizona, University of Arizona, 97 p., available at <http://www.geo.arizona.edu/Antevs/Theses/QuintanarMS08.pdf>.
- Roddick, J.C., 1983, High precision calibration of  $^{40}\text{Ar}/^{39}\text{Ar}$  standards: *Geochimica et Cosmochimica Acta*, v. 47, no. 5, p. 887-898, available at <http://www.sciencedirect.com/science/article/pii/0016703783901540>.

## **6 The Caborca Orogenic Gold Belt of Sonora, Mexico: Mica $^{40}\text{Ar}/^{39}\text{Ar}$ Geochronology from Gold-Rich Veins**

- Snee, L.W., Sutter, J.F., and Kelly, W.C., 1988, Thermochronology of economic mineral deposits; dating the stages of mineralization at Panasqueira, Portugal, by high precision  $^{40}\text{Ar}/^{39}\text{Ar}$  age spectrum techniques on muscovite: *Economic Geology*, v. 83, no. 2, p. 335–354.
- Staudacher, T., Jessberger, E.K., Dörflinger, D., and Kiko, J., 1978, A refined ultrahigh-vacuum furnace for rare gas analysis: *Journal of Physics E, Scientific Instrumentation*, v. 11, no. 8, p. 781–784.
- Steiger, R.H., and Jäger, E., 1977, Subcommittee on geochronology; convention on the use of decay constants in geo- and cosmo-chronology: *Earth and Planetary Science Letters*, v. 36, no. 3, p. 359–363, available at <http://citeseerx.ist.psu.edu/viewdoc/download?doi=10.1.1.456.667&rep=rep1&type=pdf>.

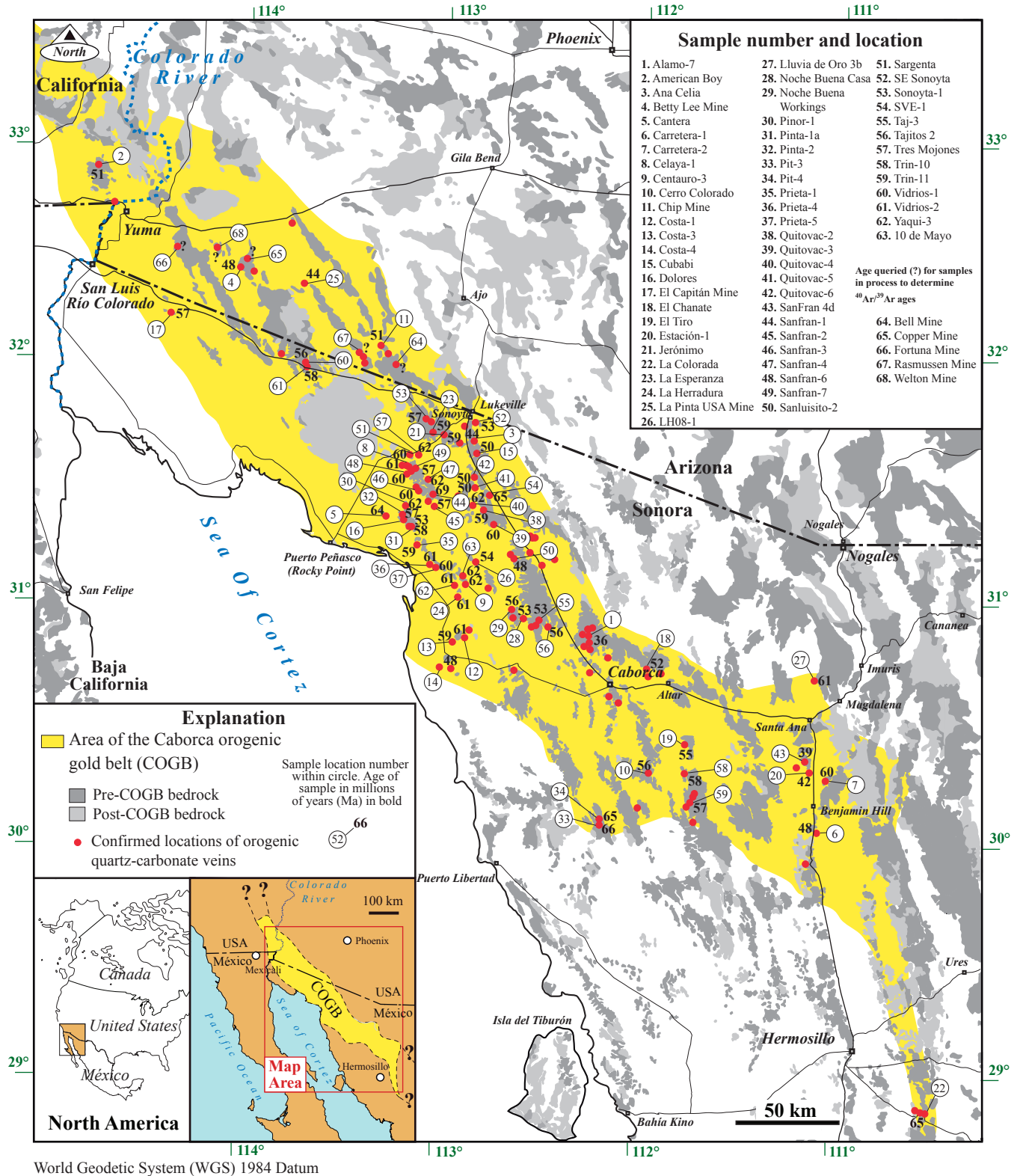


**Figure 1.** Sample locations for dated white micas of gold-rich quartz veins. Numbers in bold represent  $^{40}\text{Ar}/^{39}\text{Ar}$  ages determined in this open-file report from the Caborca orogenic gold belt (COGB), northwestern Sonora, Mexico. Shades of gray represent pre-COGB mineralization (dark-gray) and post-COGB mineralization (light-gray) bedrock outcrops after Iriondo (2001).

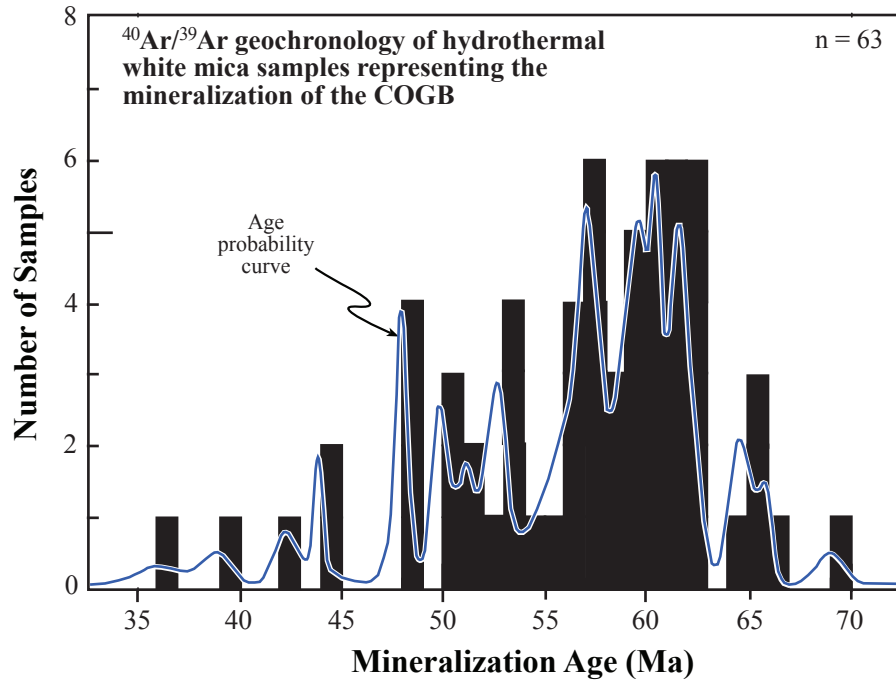


**Figure 2.** Histogram and cumulative probability distribution diagram (blue line) of  $^{40}\text{Ar}/^{39}\text{Ar}$  ages determined from hydrothermal white mica samples of gold-rich quartz veins from the Caborca orogenic gold belt (COGB), northwestern Sonora, Mexico. Abbreviations: Ma, mega-annum; n, number of samples.

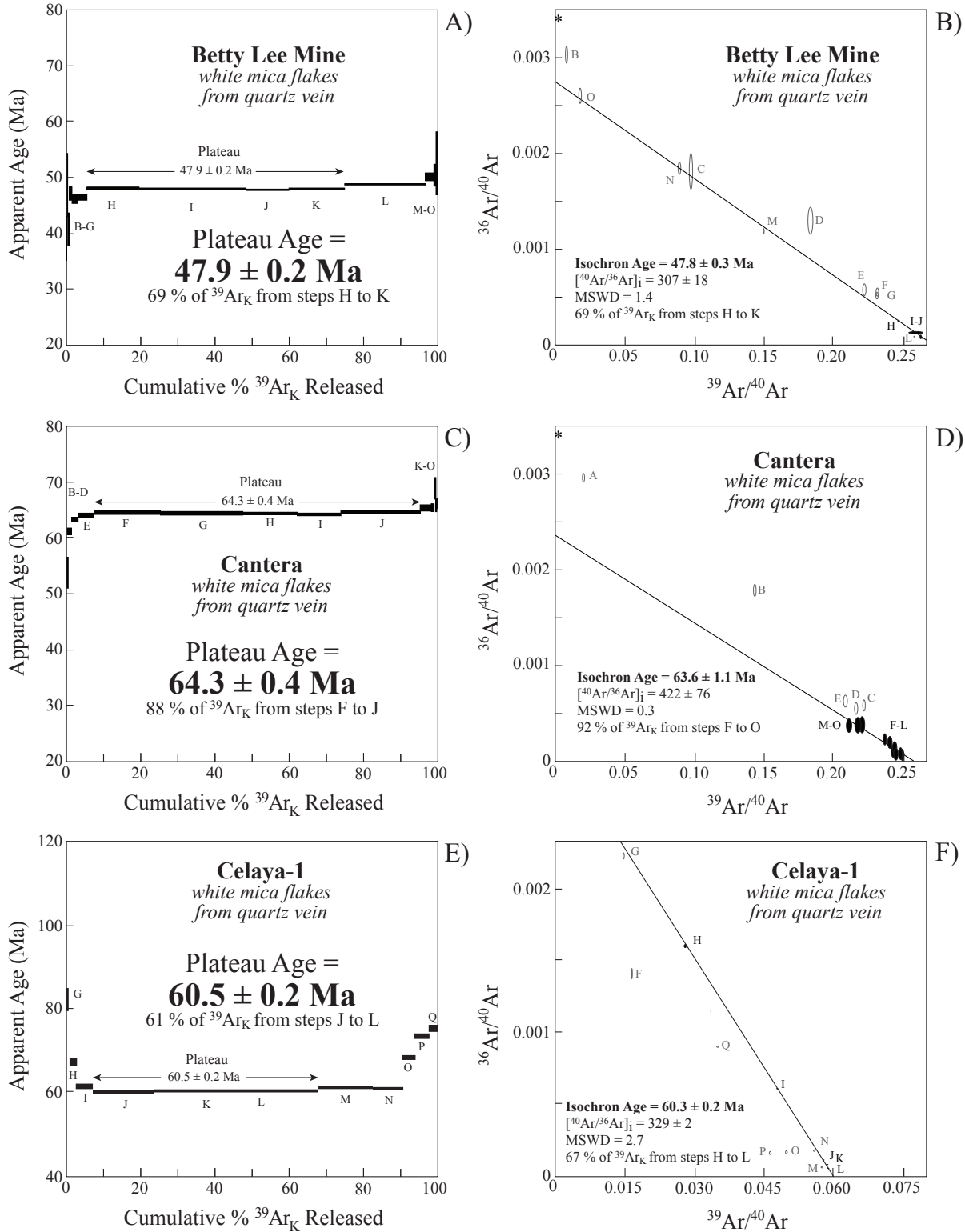


**Figure 3.** Age spectra (A, C, E) and inverse-isotope correlation diagrams (B, D, F) from group 1 of white mica samples of gold-rich quartz veins, with plateau ages as best age, from the Caborca orogenic gold belt (COGB), northwestern Sonora, Mexico. \* is the assumed limit of the atmospheric argon ratio. Abbreviations: Ma, mega-annum; MSWD, mean square weighted deviation.

10 The Caborca Orogenic Gold Belt of Sonora, Mexico: Mica  $^{40}\text{Ar}/^{39}\text{Ar}$  Geochronology from Gold-Rich Veins

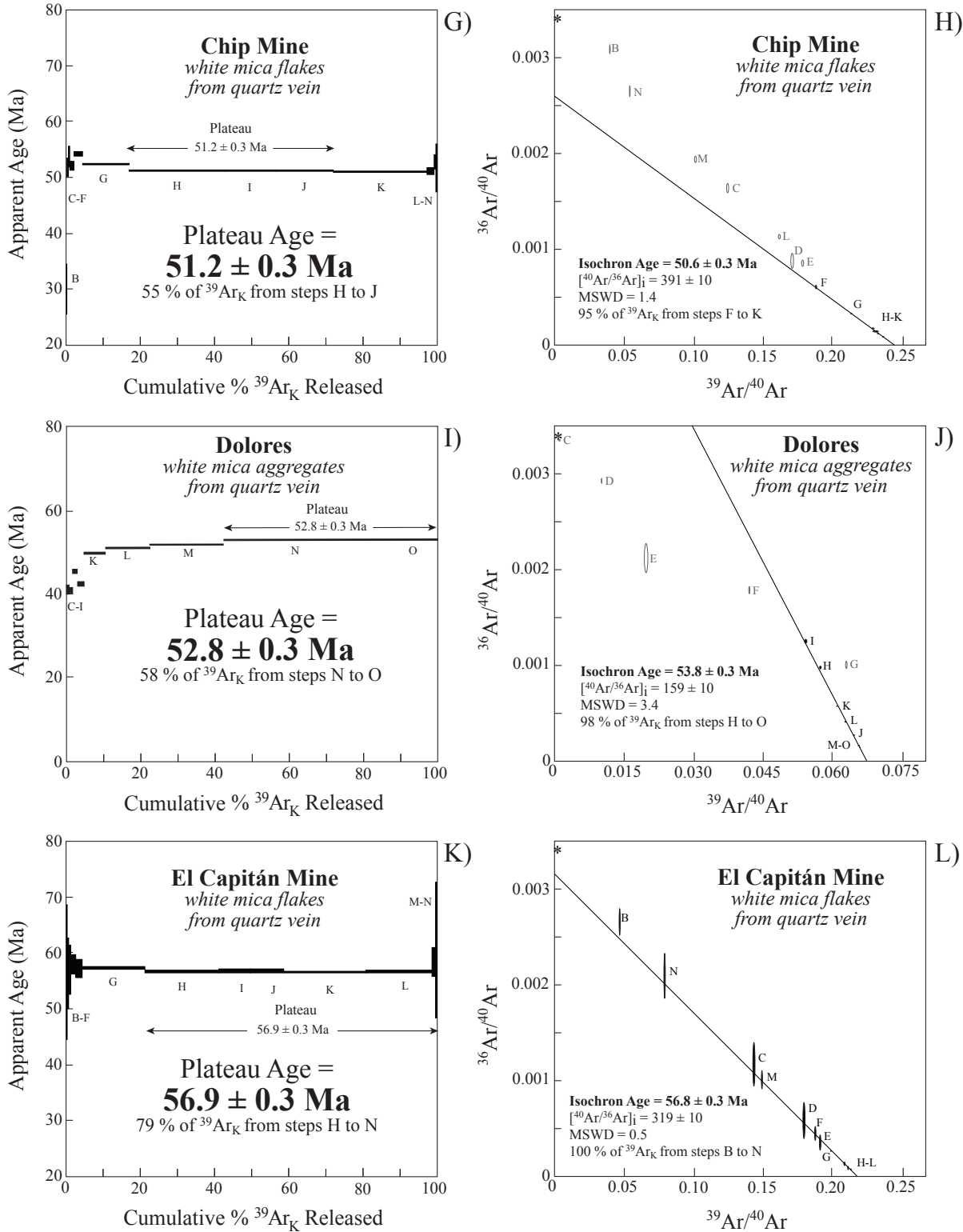
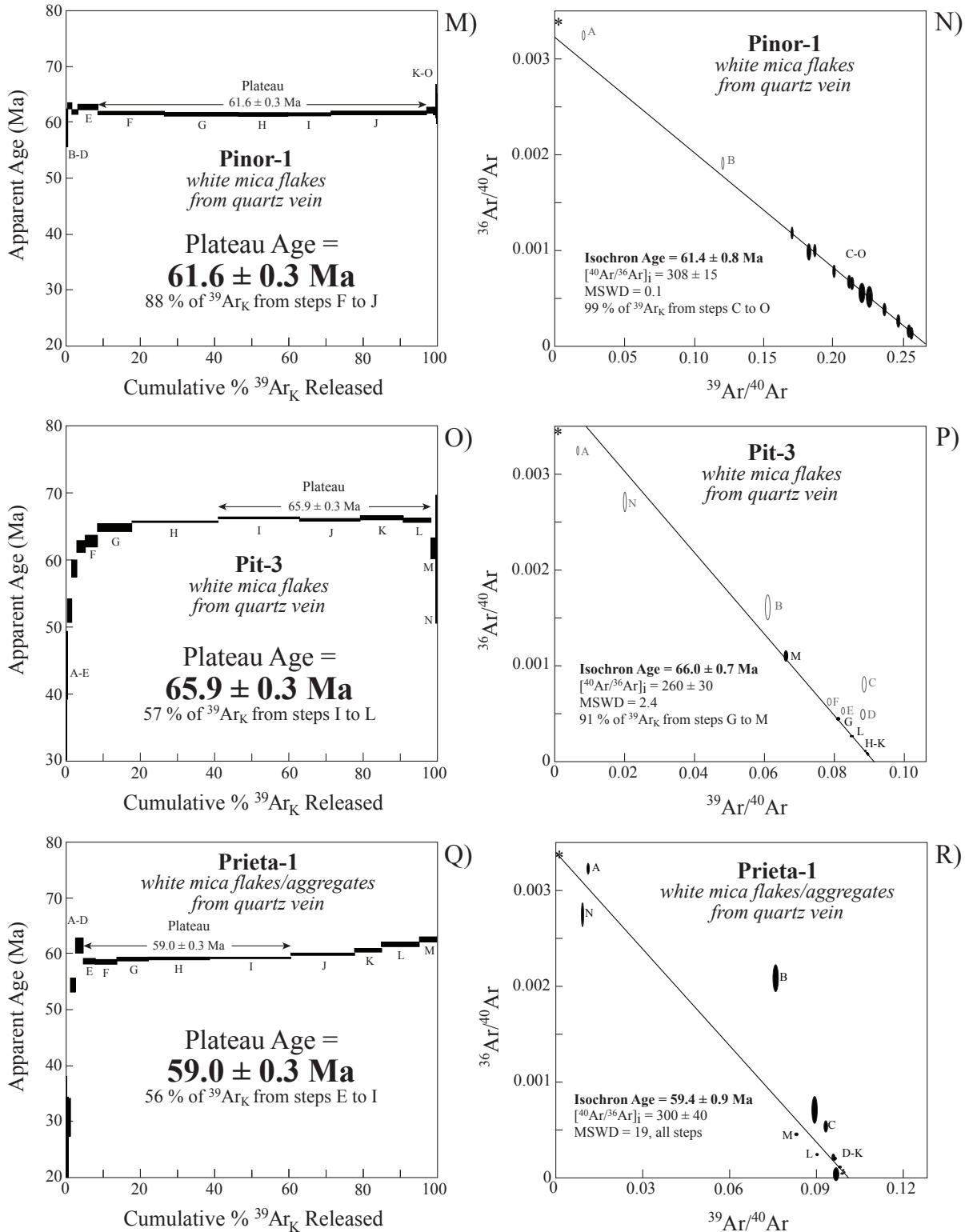


Figure 3—Continued. Age spectra (G, I, K) and inverse-isotope correlation diagrams (H, J, L) from group 1 of white mica samples of gold-rich quartz veins, with plateau ages as best age, from the Caborca orogenic gold belt (COGB), northwestern Sonora, Mexico. \* is the assumed limit of the atmospheric argon ratio.



**Figure 3—Continued.** Age spectra (M, O, Q) and inverse-isotope correlation diagrams (N, P, R) from group 1 of white mica samples of gold-rich quartz veins, with plateau ages as best age, from the Caborca orogenic gold belt (COGB), northwestern Sonora, Mexico. \* is the assumed limit of the atmospheric argon ratio.

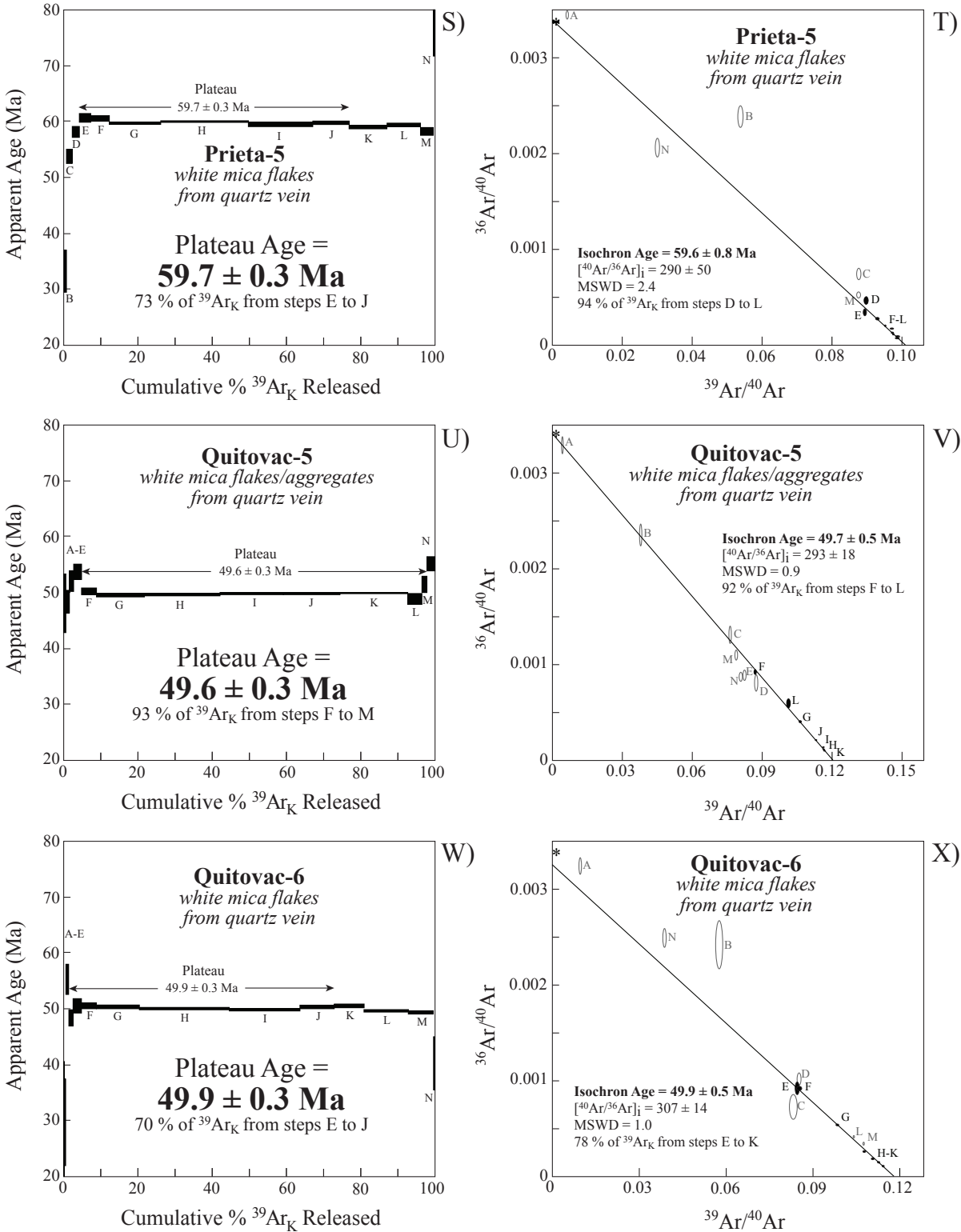
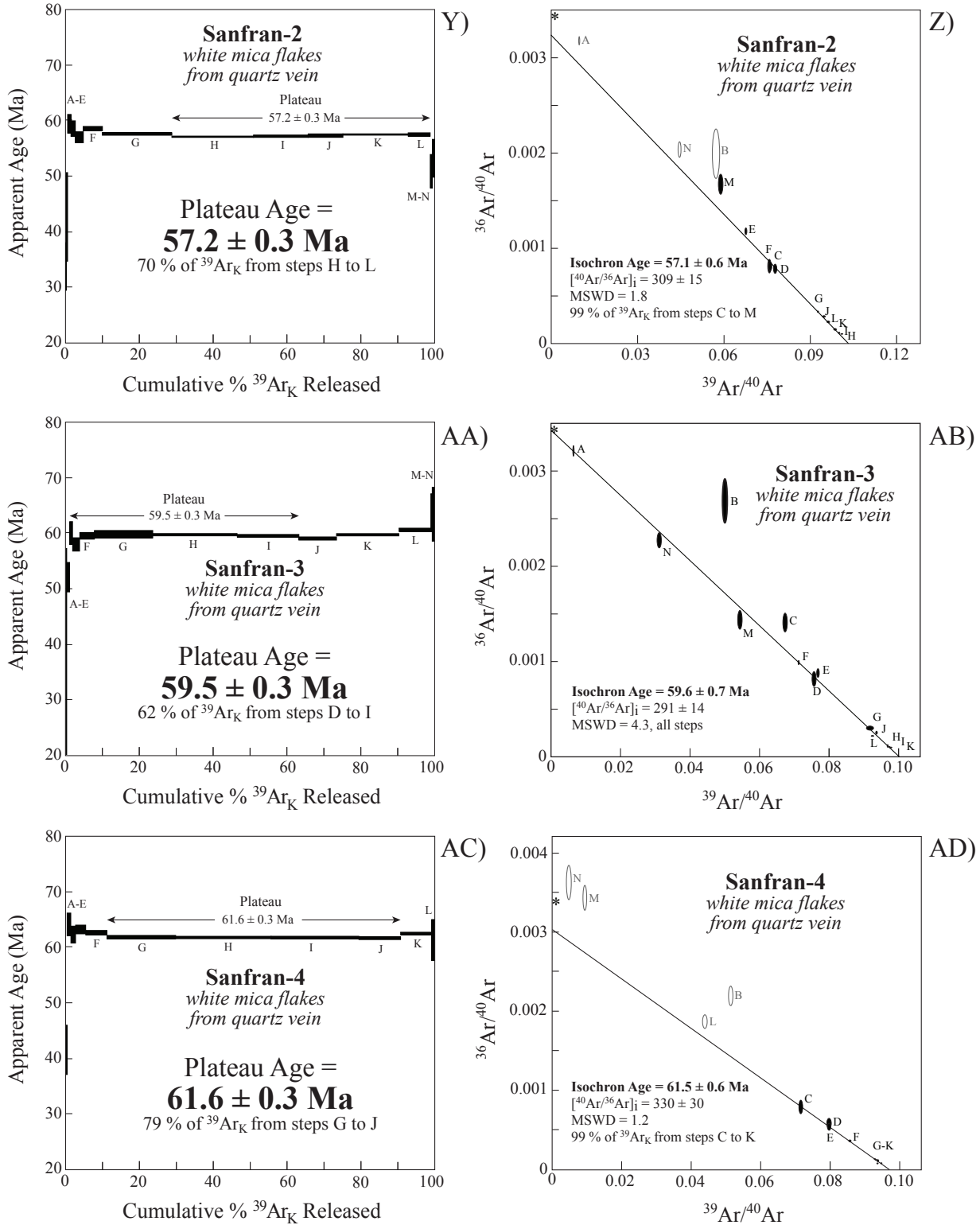


Figure 3—Continued. Age spectra (S, U, W) and inverse-isotope correlation diagrams (T, V, X) from group 1 of white mica samples of gold-rich quartz veins, with plateau ages as best age, from the Caborca orogenic gold belt (COGB), northwestern Sonora, Mexico. \* is the assumed limit of the atmospheric argon ratio.



**Figure 3—Continued.** Age spectra (Y, AA, AC) and inverse-isotope correlation diagrams (Z, AB, AD) from group 1 of white mica samples of gold-rich quartz veins, with plateau ages as best age, from the Caborca orogenic gold belt (COGB), northwestern Sonora, Mexico. \* is the assumed limit of the atmospheric argon ratio.

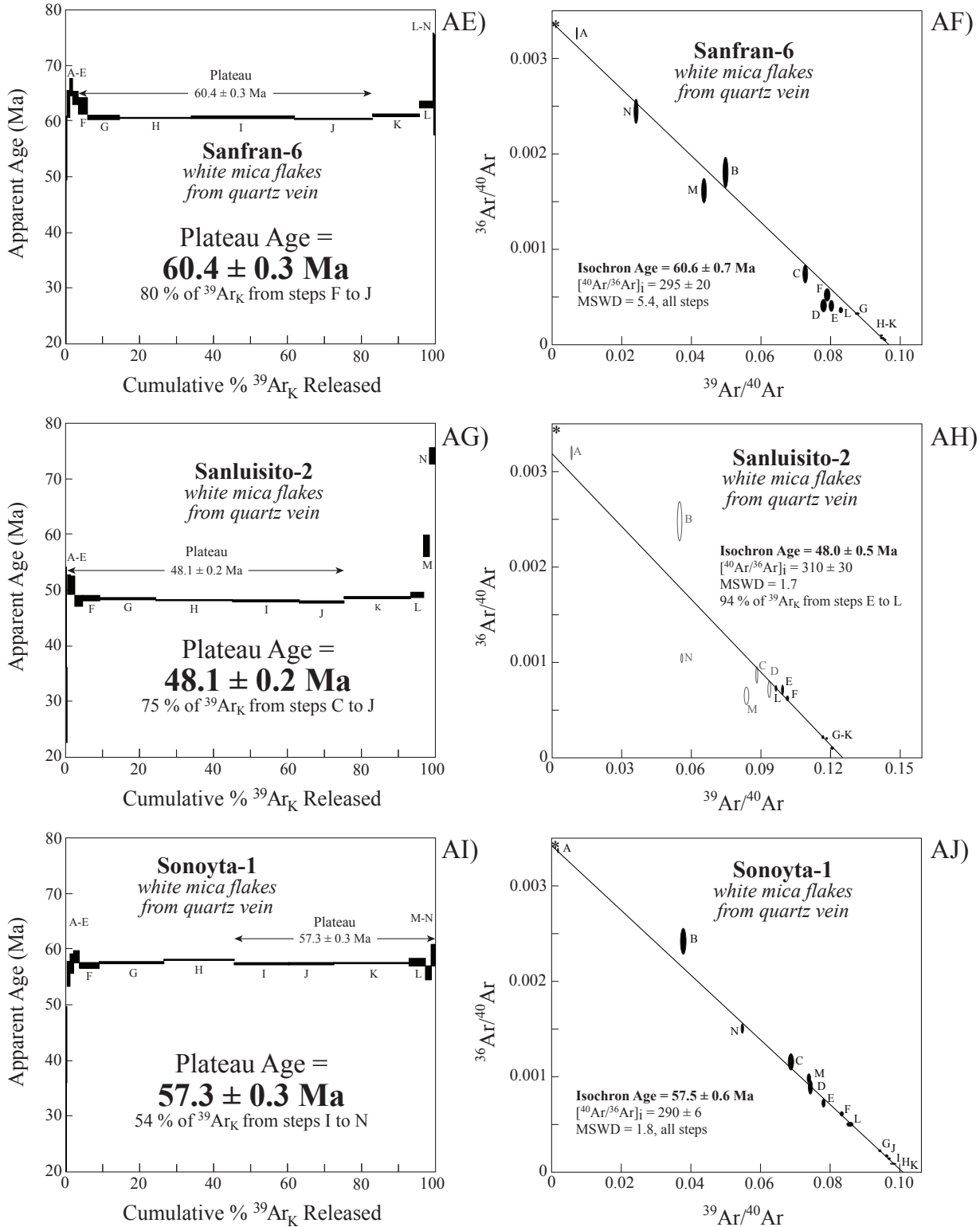
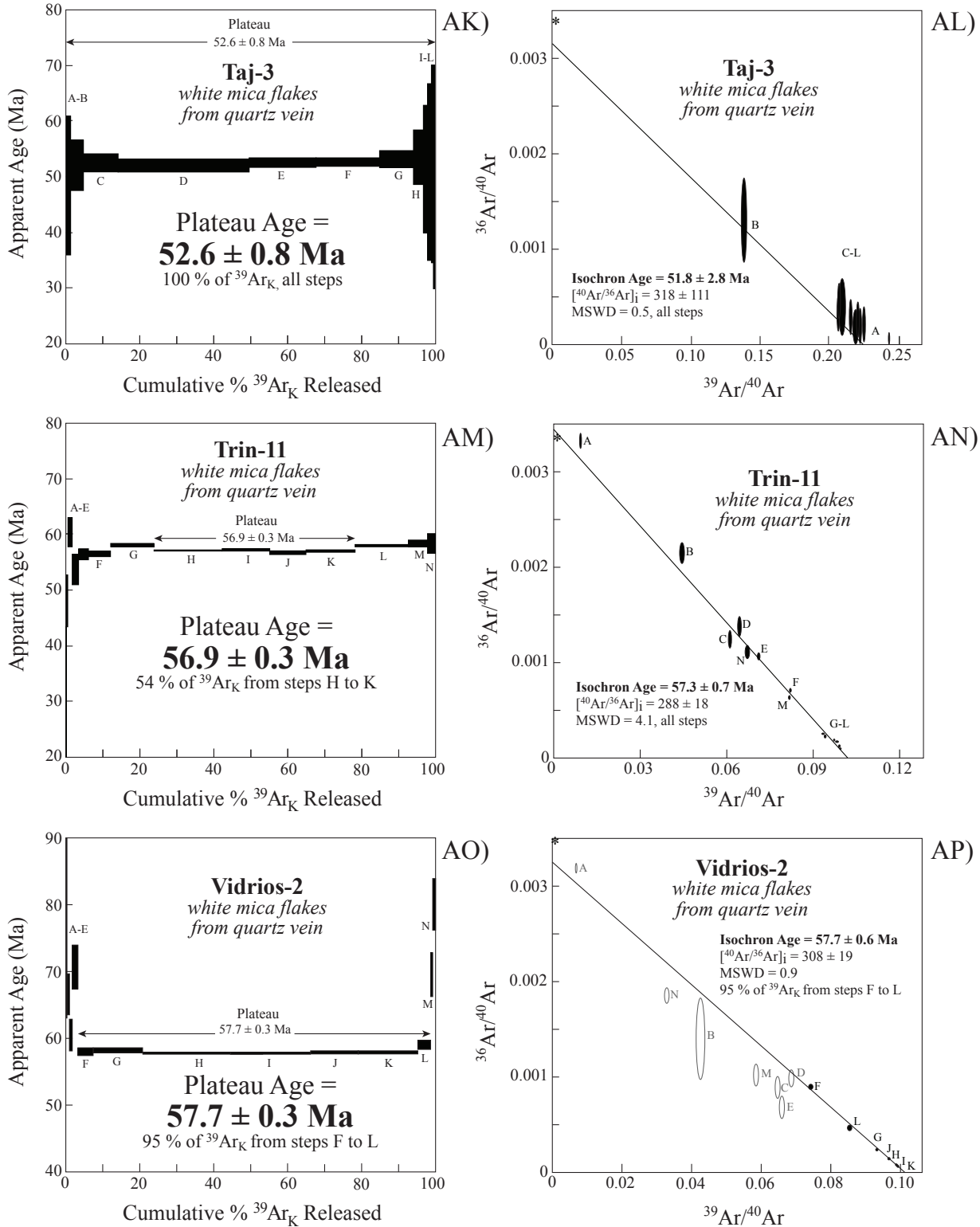
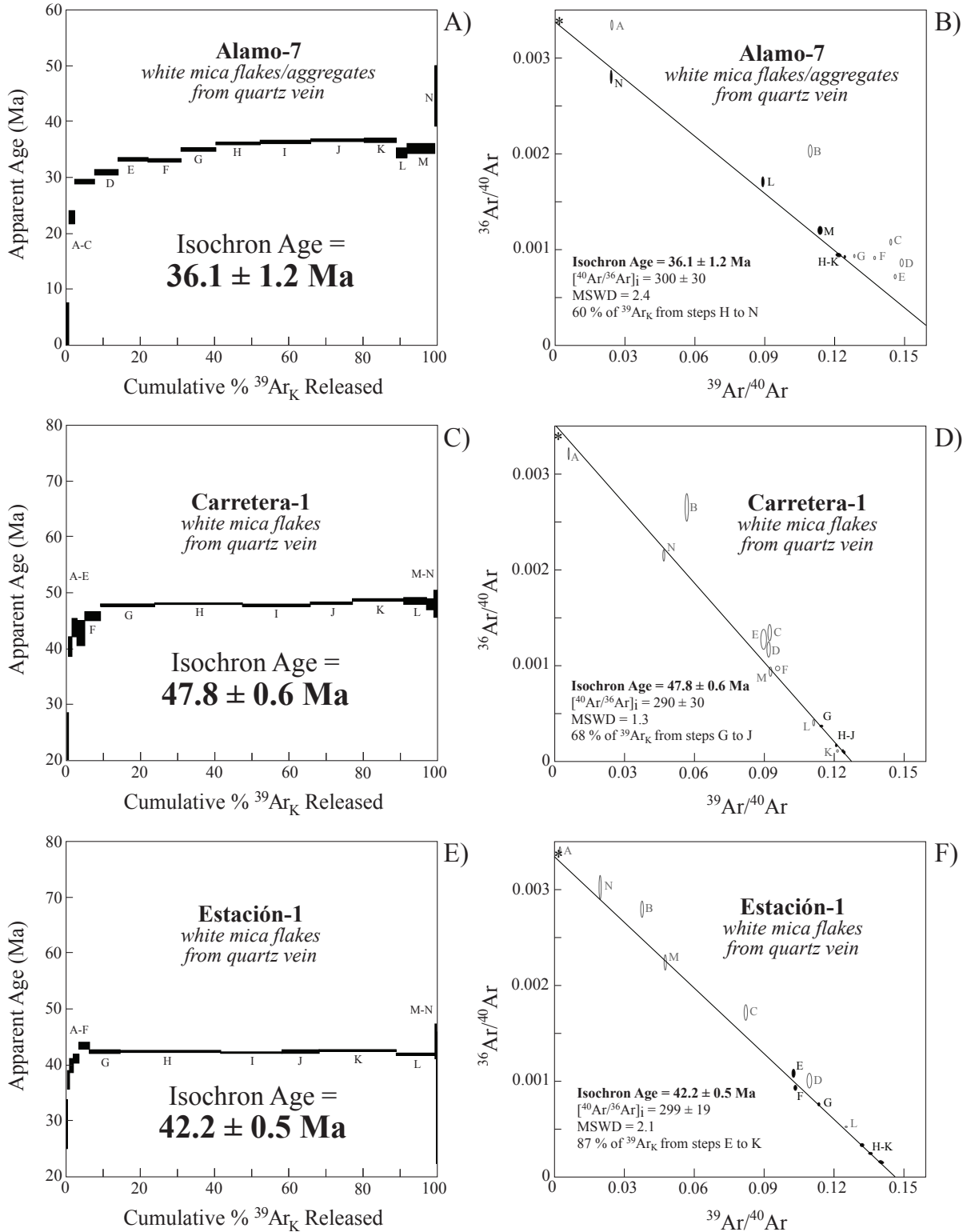


Figure 3—Continued. Age spectrum (AE, AG, AI) and inverse-isotope correlation diagrams (AF, AH, AJ) from group 1 of white mica samples of gold-rich quartz veins, with plateau age as best age, from the Caborca orogenic gold belt (COGB), northwestern Sonora, Mexico. \* is the assumed limit of the atmospheric argon ratio.



**Figure 3—Continued.** Age spectrum (AK, AM, AO) and inverse-isotope correlation diagrams (AL, AN, AP) from group 1 of white mica samples of gold-rich quartz veins, with plateau age as best age, from the Caborca orogenic gold belt (COGB), northwestern Sonora, Mexico. \* is the assumed limit of the atmospheric argon ratio.



**Figure 4.** Age spectra (A, C, E) and inverse-isotope correlation diagrams (B, D, F) from group 2 of white mica samples of gold-rich quartz veins, with isochron ages as best age, from the Caborca orogenic gold belt (COGB), northwestern Sonora, Mexico. \* is the assumed limit of the atmospheric argon ratio. Abbreviations: Ma, mega-annum; MSWD, mean square weighted deviation.

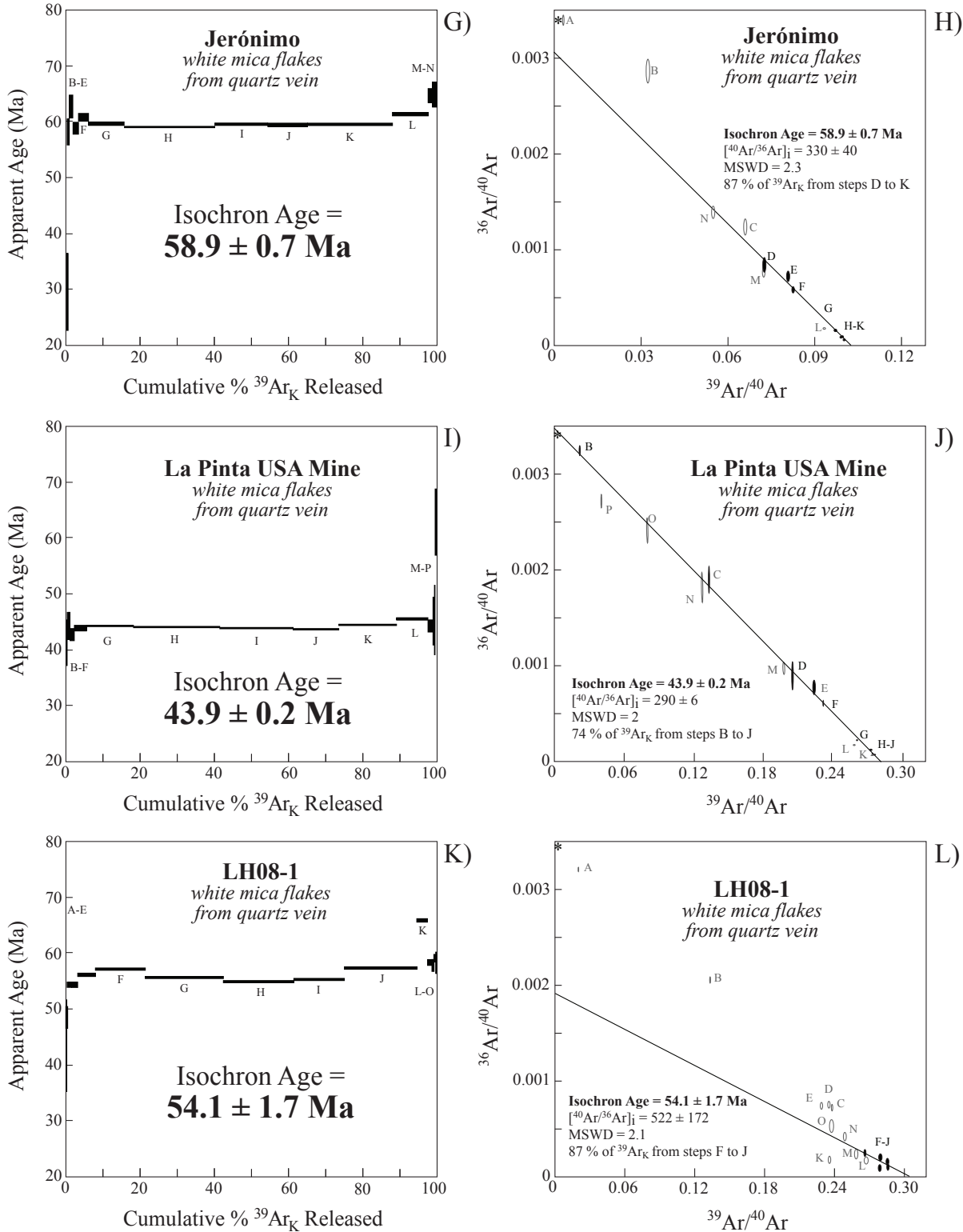


**Figure 4—Continued.** Age spectra (G, I, K) and inverse-isotope correlation diagrams (H, J, L) from group 2 of white mica samples of gold-rich quartz veins, with isochron ages as best age, from the Caborca orogenic gold belt (COGB), northwestern Sonora, Mexico. \* is the assumed limit of the atmospheric argon ratio.

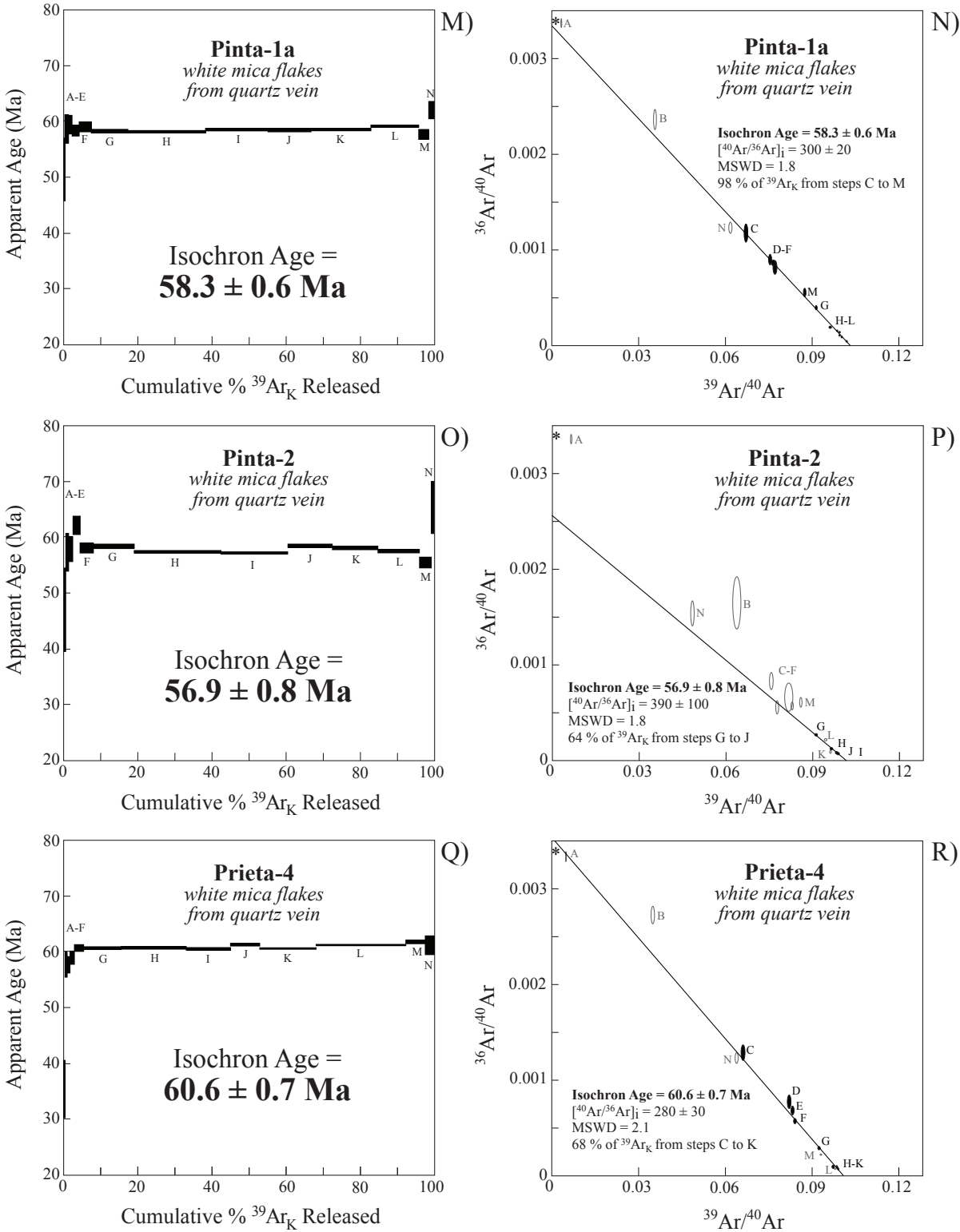
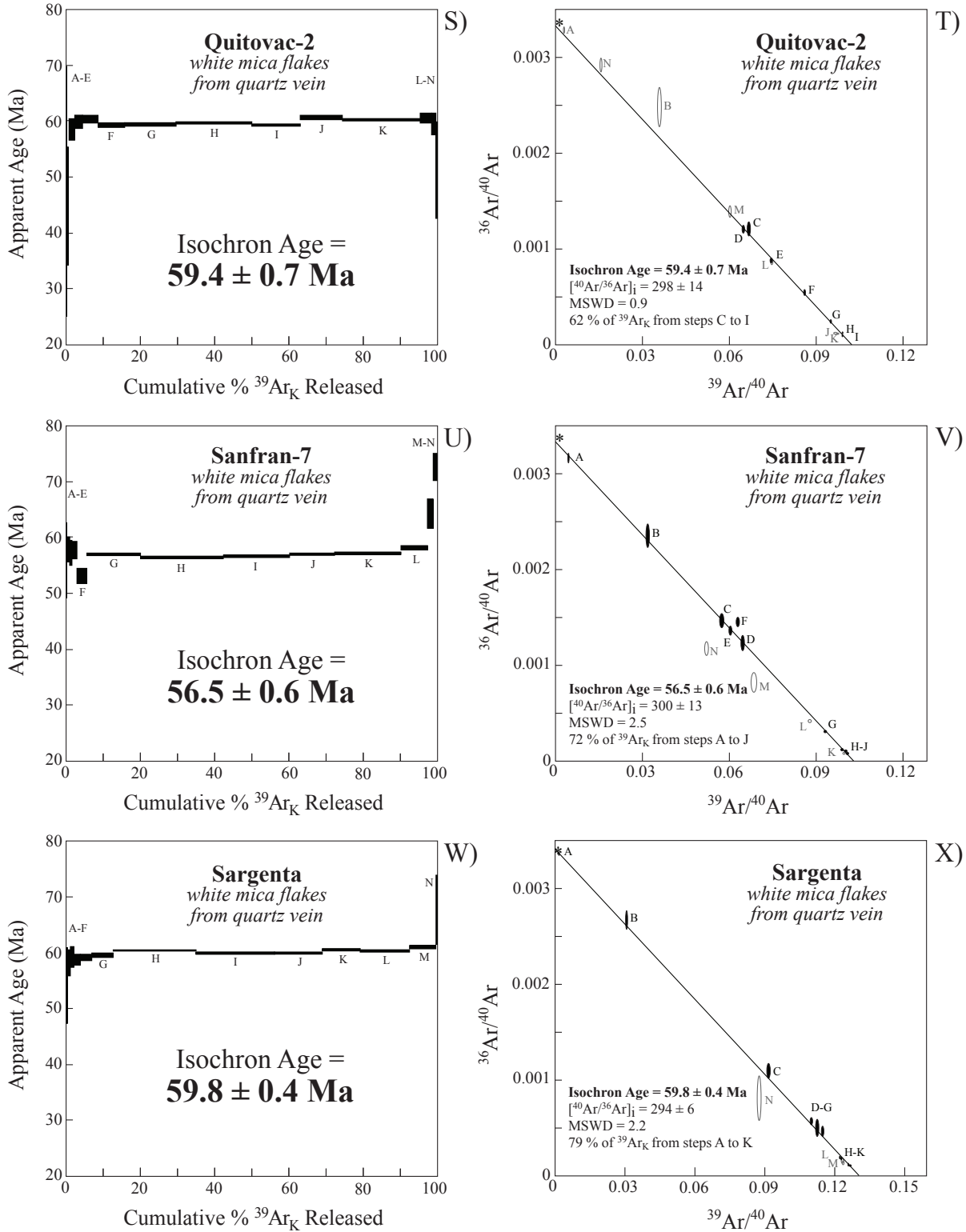


Figure 4—Continued. Age spectra (M, O, Q) and inverse-isotope correlation diagrams (N, P, R) from group 2 of white mica samples of gold-rich quartz veins, with isochron ages as best age, from the Caborca orogenic gold belt (COGB), northwestern Sonora, Mexico. \* is the assumed limit of the atmospheric argon ratio.



**Figure 4—Continued.** Age spectra (S, U, W) and inverse-isotope correlation diagrams (T, V, X) from group 2 of white mica samples of gold-rich quartz veins, with isochron ages as best age, from the Caborca orogenic gold belt (COGB), northwestern Sonora, Mexico. \* is the assumed limit of the atmospheric argon ratio.

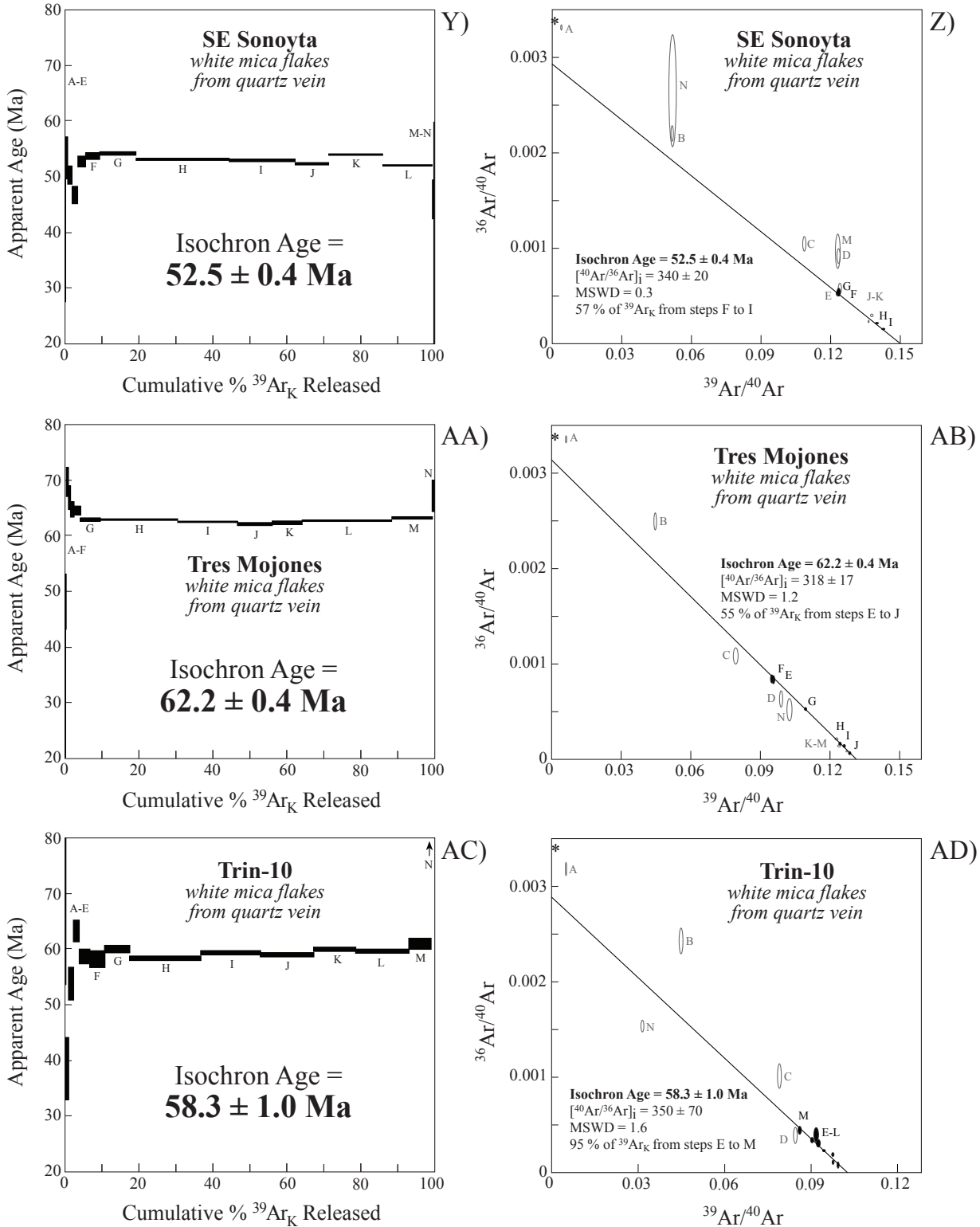
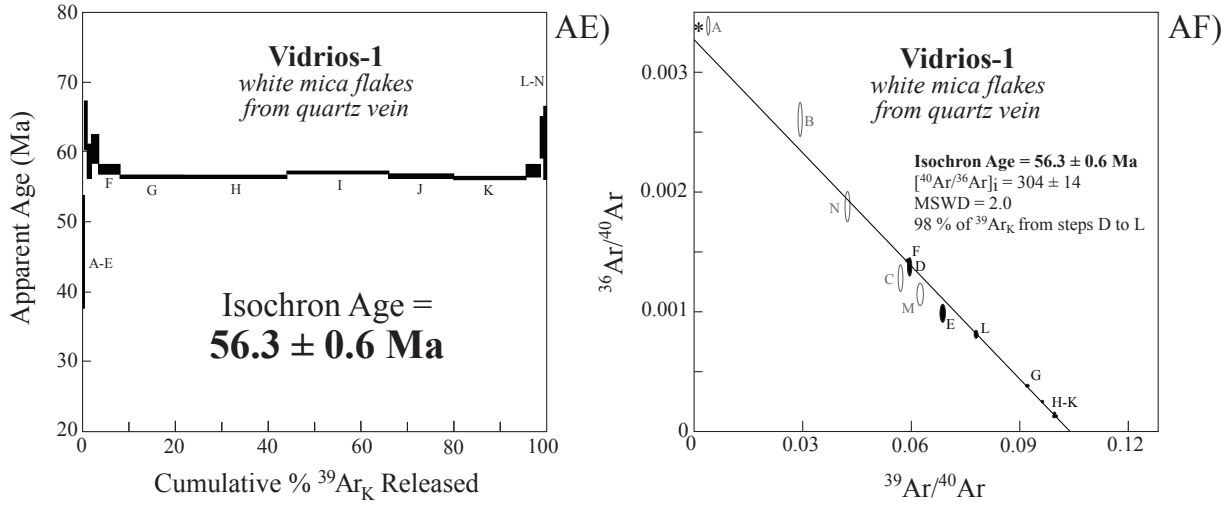
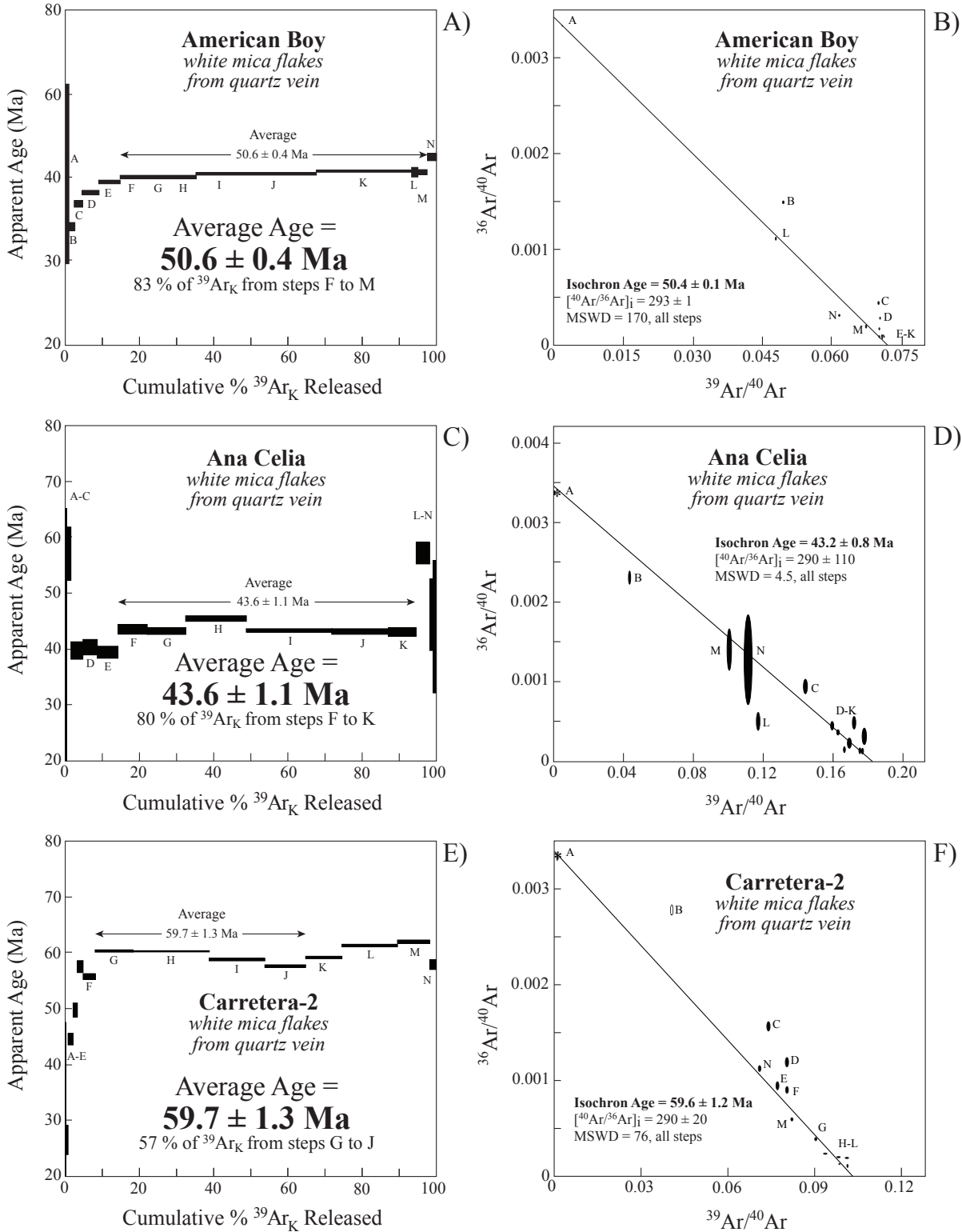


Figure 4—Continued. Age spectra (Y, AA, AC) and inverse-isotope correlation diagrams (Z, AB, AD) from group 2 of white mica samples of gold-rich quartz veins, with isochron ages as best age, from the Caborca orogenic gold belt (COGB), northwestern Sonora, Mexico. \* is the assumed limit of the atmospheric argon ratio.



**Figure 4—Continued.** Age spectra (AE) and inverse-isotope correlation diagrams (AF) from group 2 of white mica samples of gold-rich quartz veins, with isochron ages as best age, from the Caborca orogenic gold belt (COGB), northwestern Sonora, Mexico. \* is the assumed limit of the atmospheric argon ratio.



**Figure 5.** Age spectra (A, C, E) and inverse-isotope correlation diagrams (B, D, F) from group 3 of white mica samples of gold-rich quartz veins, with average ages as best age, from the Caborca orogenic gold belt (COGB), northwestern Sonora, Mexico. \* is the assumed limit of the atmospheric argon ratio. Abbreviations: Ma, mega-annum; MSWD, mean square weighted deviation.

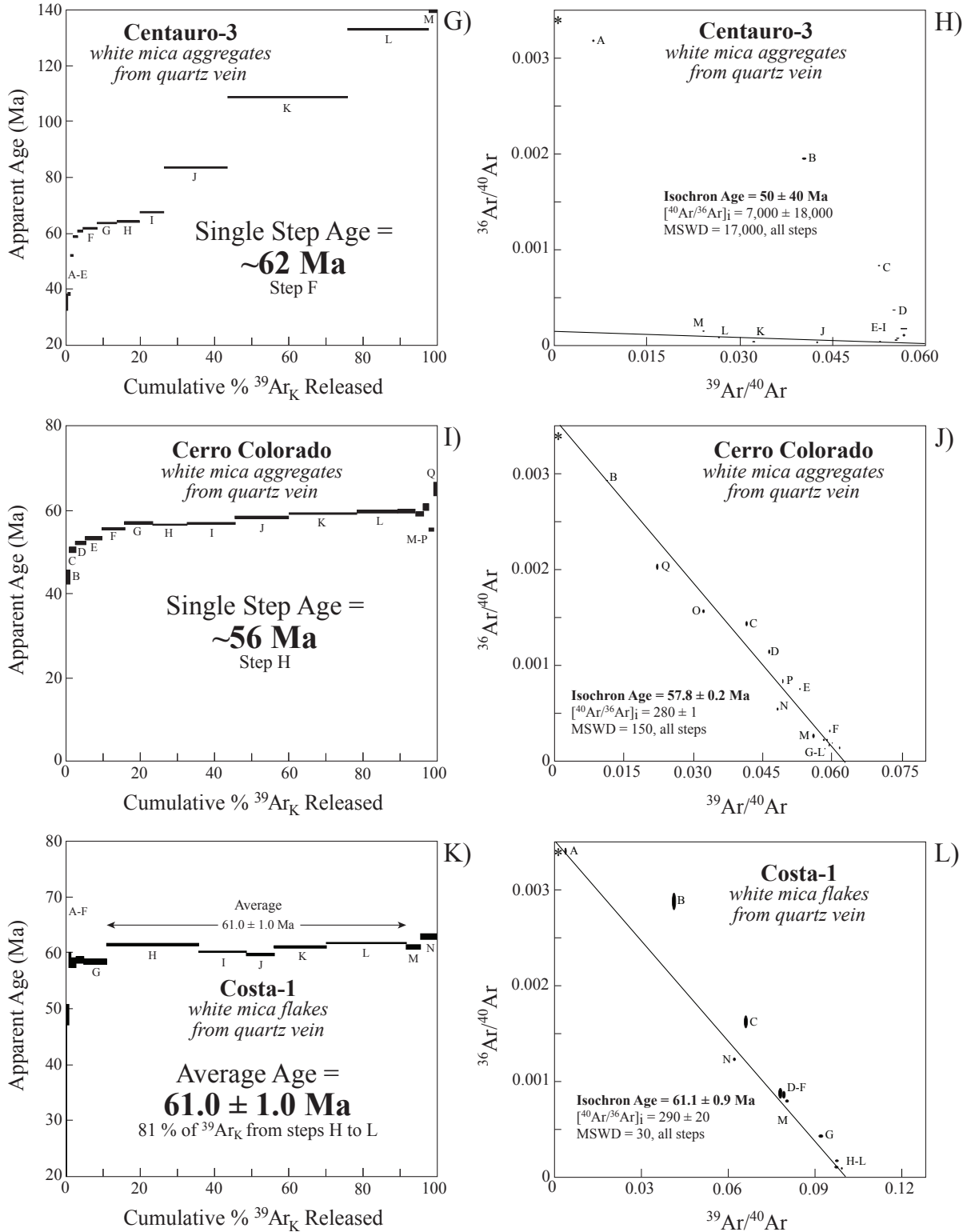


**Figure 5—Continued.** Age spectra (G, I, K) and inverse-isotope correlation diagrams (H, J, L) from group 3 of white mica samples of gold-rich quartz veins, with average and single-step ages as best age, from the Caborca orogenic gold belt (COGB), northwestern Sonora, Mexico. \* is the assumed limit of the atmospheric argon ratio.

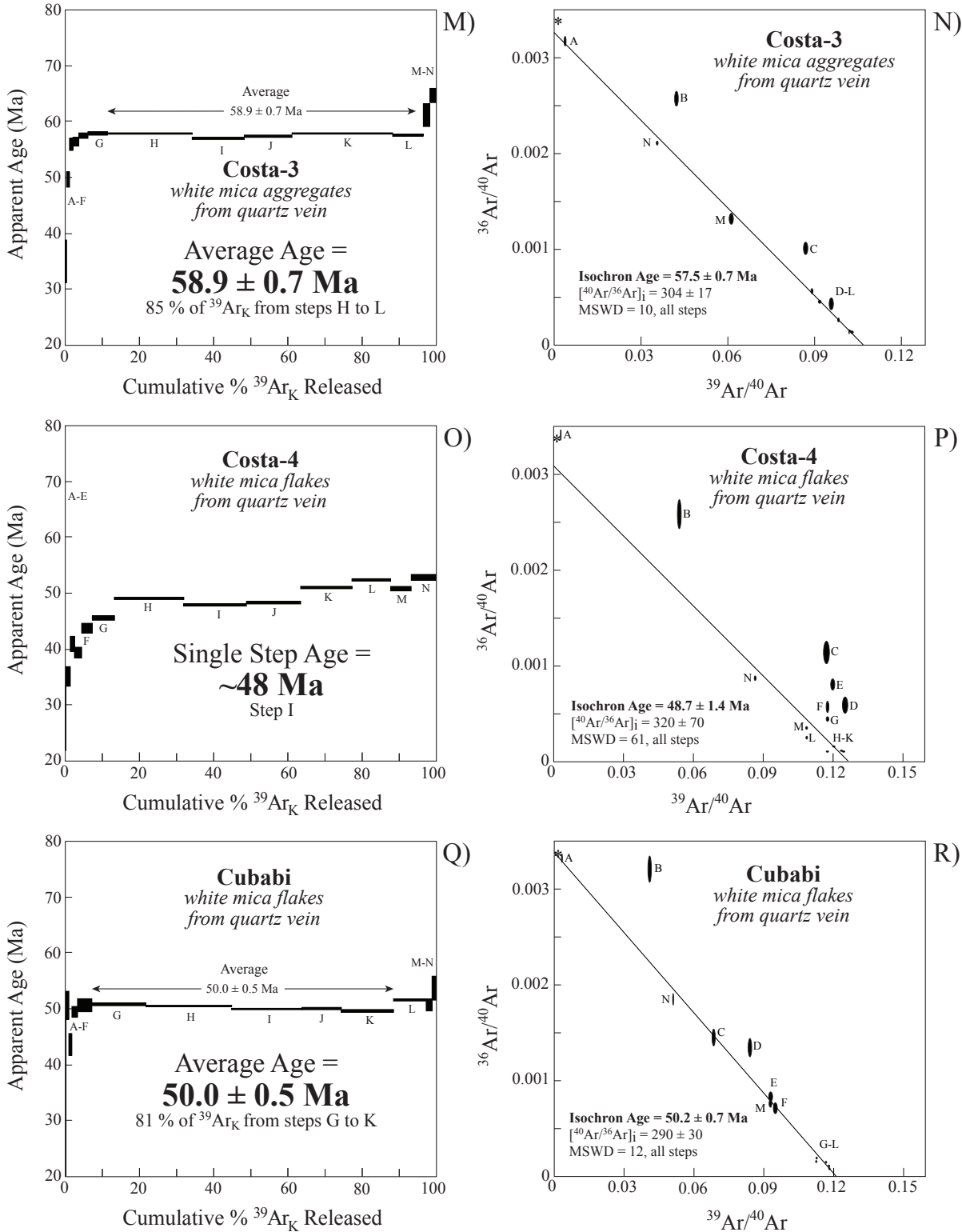
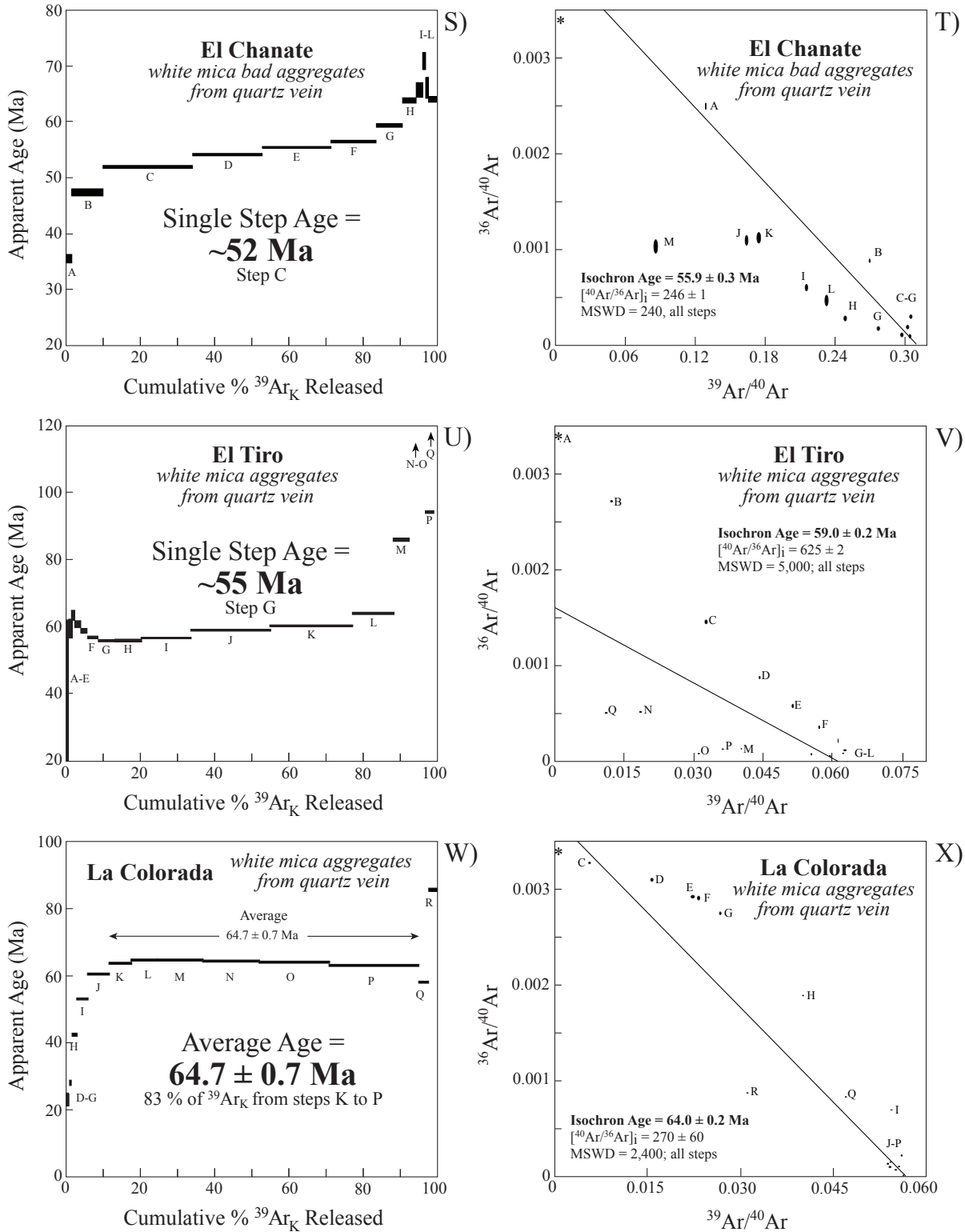


Figure 5—Continued. Age spectra (M, O, Q) and inverse-isotope correlation diagrams (N, P, R) from group 3 of white mica samples of gold-rich quartz veins, with average and single-step ages as best age, from the Caborca orogenic gold belt (COGB), northwestern Sonora, Mexico. \* is the assumed limit of the atmospheric argon ratio.



**Figure 5—Continued.** Age spectra (S, U, W) and inverse-isotope correlation diagrams (T, V, X) from group 3 of white mica samples of gold-rich quartz veins, with average and single-step ages as best age, from the Caborca orogenic gold belt (COGB), northwestern Sonora, Mexico. \* is the assumed limit of the atmospheric argon ratio.

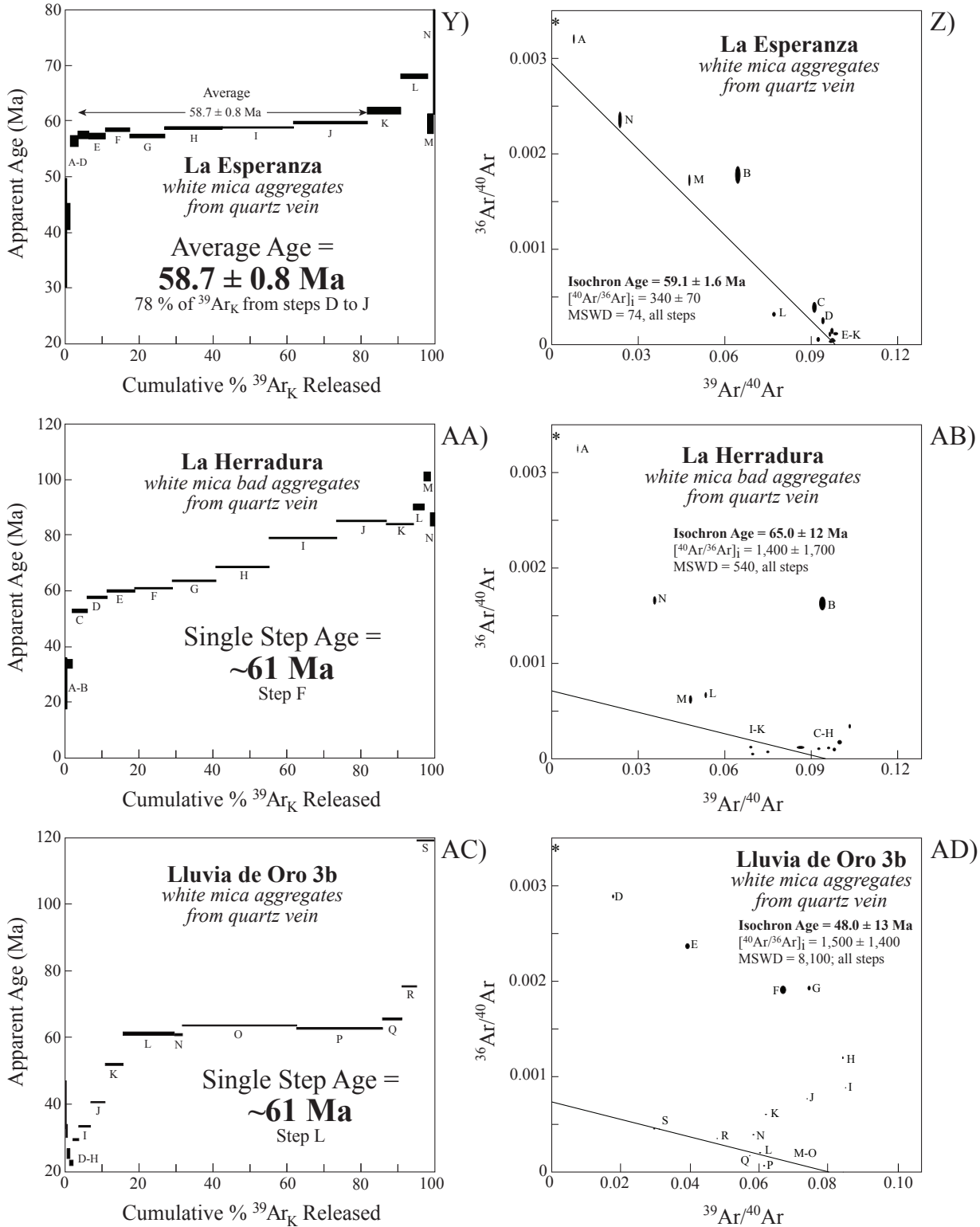
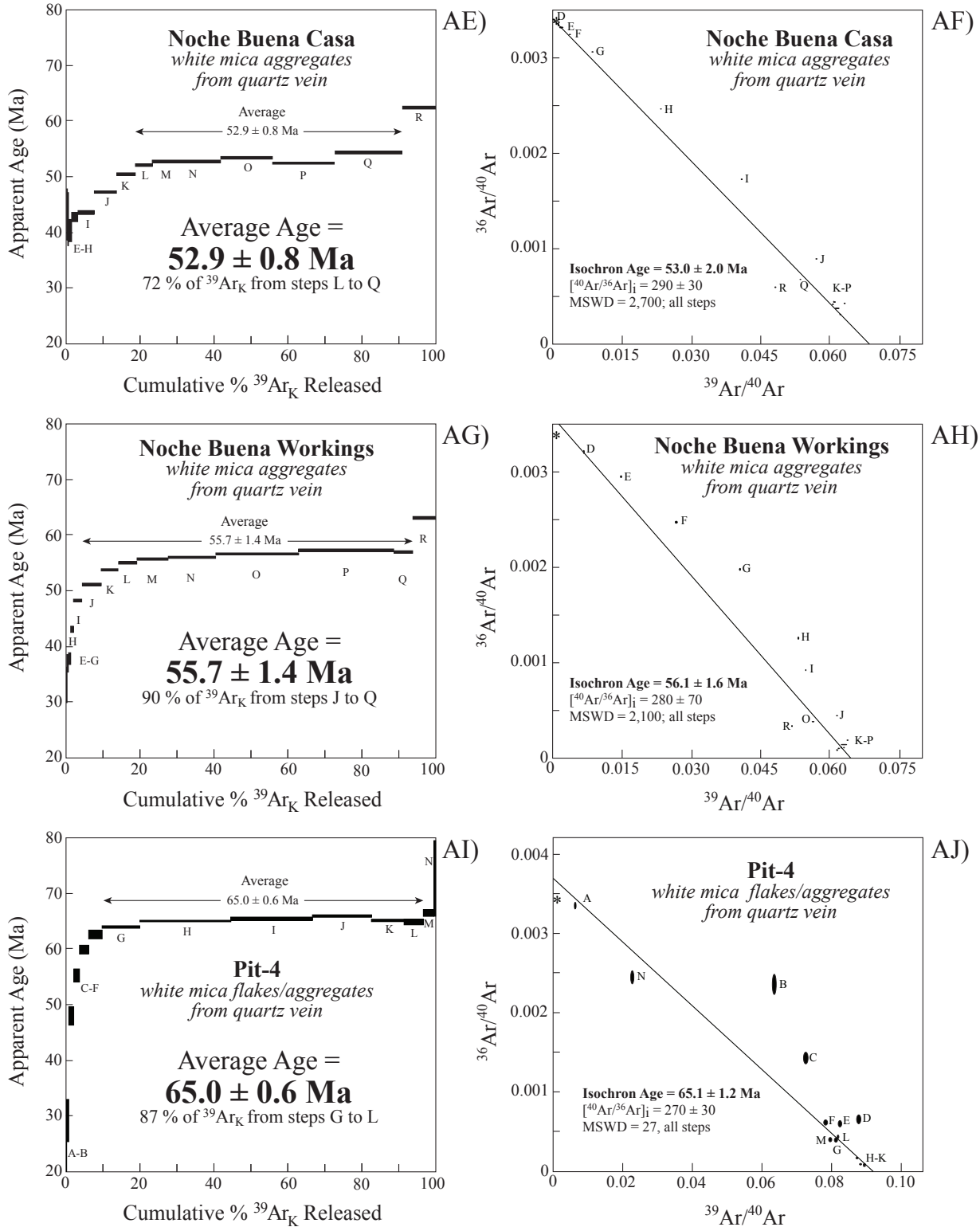


Figure 5—Continued. Age spectra (Y, AA, AC) and inverse-isotope correlation diagrams (Z, AB, AD) from group 3 of white mica samples of gold-rich quartz veins, with average and single-step ages as best age, from the Caborca orogenic gold belt (COGB), northwestern Sonora, Mexico. \* is the assumed limit of the atmospheric argon ratio.



**Figure 5—Continued.** Age spectra (AE, AG, AI) and inverse-isotope correlation diagrams (AF, AH, AJ) from group 3 of white mica samples of gold-rich quartz veins, with average ages as best age, from the Caborca orogenic gold belt (COGB), northwestern Sonora, Mexico. \* is the assumed limit of the atmospheric argon ratio.

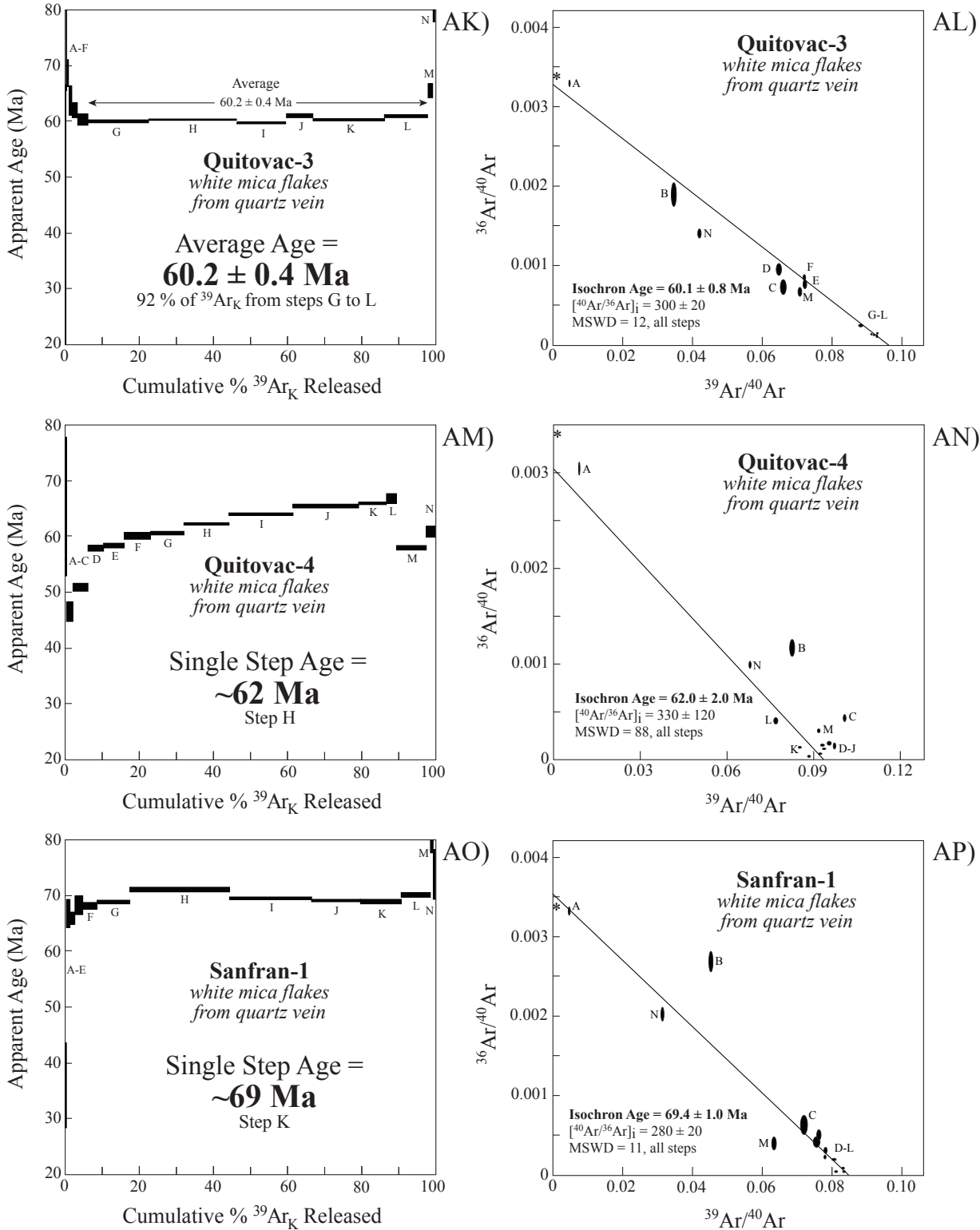
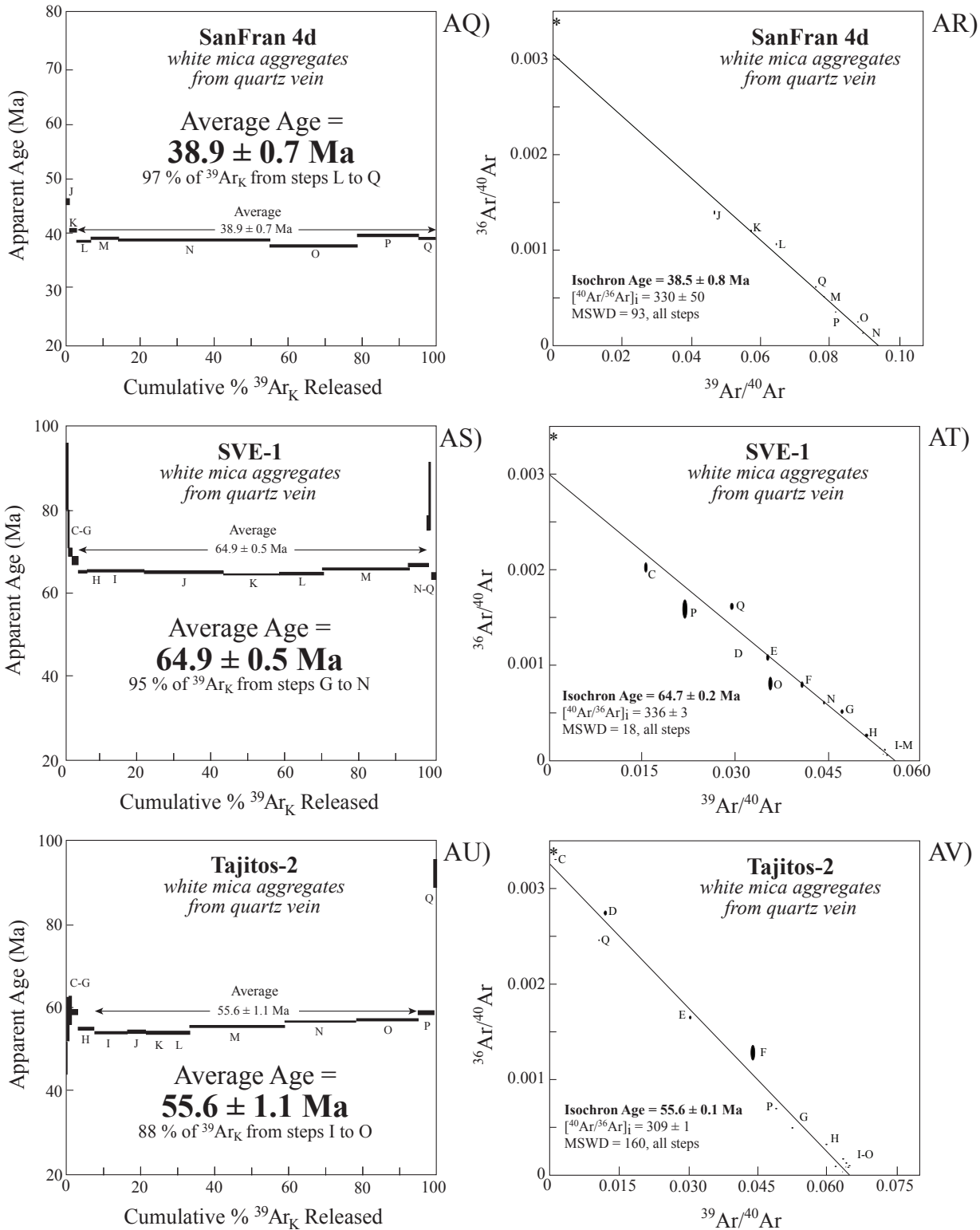


Figure 5—Continued. Age spectra (AK, AM, AO) and inverse-isotope correlation diagrams (AL, AN, AP) from group 3 of white mica samples of gold-rich quartz veins, with average and single-step ages as best age, from the Caborca orogenic gold belt (COGB), northwestern Sonora, Mexico. \* is the assumed limit of the atmospheric argon ratio.



**Figure 5—Continued.** Age spectra (AQ, AS, AU) and inverse-isotope correlation diagrams (AR, AT, AV) from group 3 of white mica samples of gold-rich quartz veins, with average ages as best age, from the Caborca orogenic gold belt (COGB), northwestern Sonora, Mexico. \* is the assumed limit of the atmospheric argon ratio.

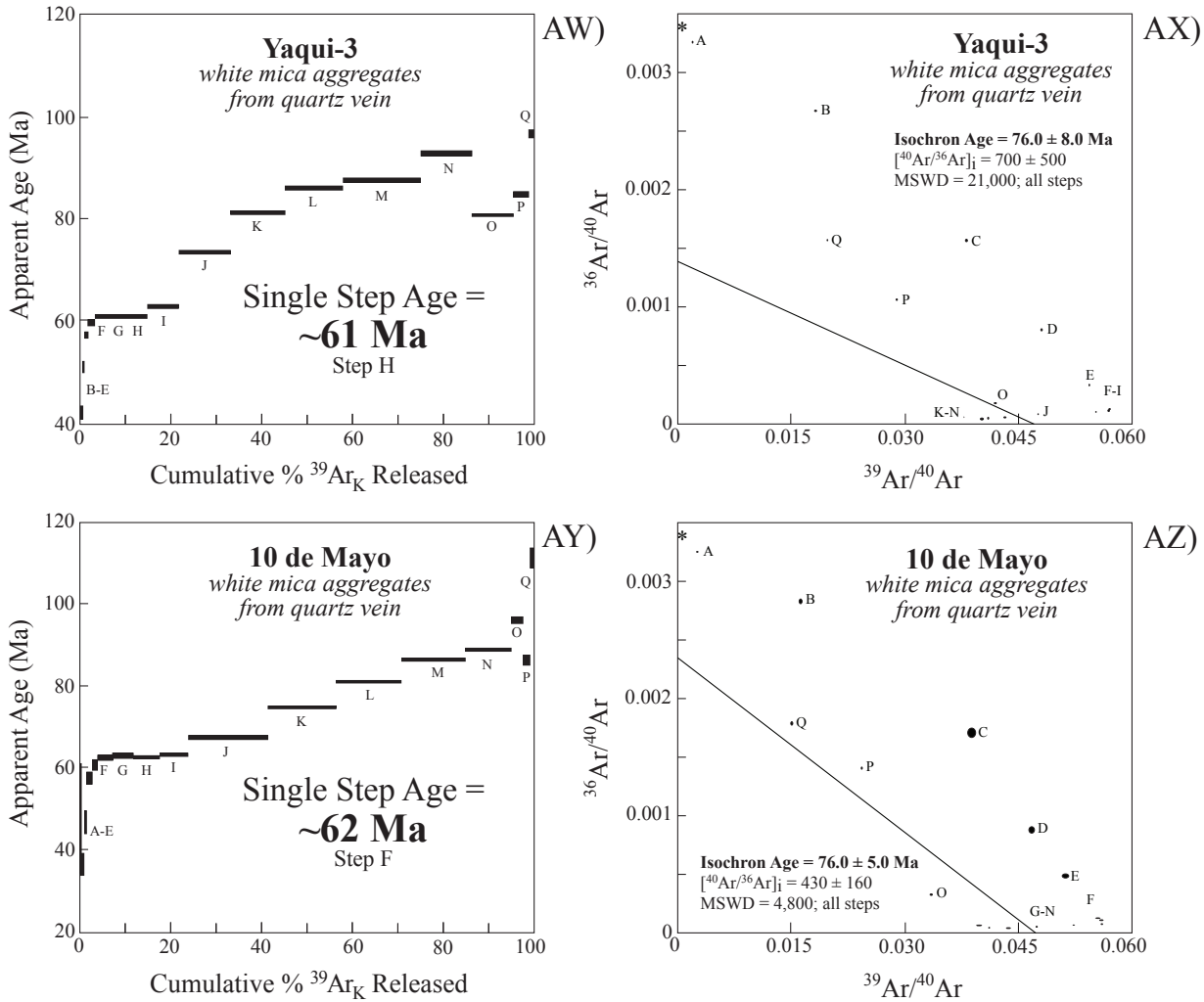


Figure 5—Continued. Age spectrum (AW, AY) and inverse-isotope correlation diagram (AX, AZ) from group 3 of white mica samples of gold-rich quartz veins, with single-step age as best age, from the Caborca orogenic gold belt (COGB), northwestern Sonora, Mexico. \* is the assumed limit of the atmospheric argon ratio.



